Norwegian University
of Life Sciences

Master's Thesis 2022 60 ECTS
Faculty of Environmental Sciences and Natural Resource Management

Factors Affecting the Water Chemistry of Non-Glaciated High Arctic Catchments: A Snapshot Study of Lake Sarsvatnet, Svalbard

Lill Katrin Gorseth
Environment and Natural Resources

This thesis was conducted in collaboration with:

UNIS

The University Centre in Svalbard

Abstract

The Arctic is warming up faster than the global average and the projected changes are believed to impact High Arctic freshwater systems. However, the consequences are poorly understood. To understand how these systems are responding to a changing climate, there is a need for baseline data. Here, a snapshot study of the water chemistry of a poorly investigated non-glaciated High Arctic catchment (Lake Sarsvatnet, Svalbard) is presented. The aim was to explore the main factors influencing these systems. With water samples from the lake and surrounding streams collected in August 2021, a picture of the freshwater chemistry was obtained including trace elements (Fe, Mn, Al, Ni, As, Co, Cu, Zn, Pb, Cd), major ions (Ca^{2+}, HCO_3^-, SO_4^{2-}, Mg^{2+}, Cl^-, Na^+, K^+), pH, conductivity, total organic carbon (TOC) and turbidity.

Lake Sarsvatnet showed similar characteristics to other Svalbard lakes. However, elevated concentrations of Cu and Zn (total of 60.74 µg/l and 43.08 µg/l respectively) were found. Through a Principal Component Analysis (PCA) and sea salt correction, most of the trace element and major ion content in the streams was found to be explained by rock weathering and inputs from marine aerosols. However, Cd in stream samples could be linked to atmospheric deposition, which nowadays may originate from mineral dust from the erosion of newly ice-free environments on Svalbard. An enrichment of Pb, Mn, Fe, Cu, Zn and Cd in Lake Sarsvatnet compared to stream samples could plausibly be explained by the inwash of minerogenic material. This could have been initiated by precipitation events, which are expected to happen more frequently with a changing climate. Moreover, further research on seasonal and multi-seasonal variations in water chemistry is recommended to better understand climate-induced changes in the Arctic.

Sammendrag

Arktis varmes opp raskere enn andre steder i verden, og de tilhørende endringene er antatt å påvirke høyarktiske ferskvannssystemer. Derimot er konsekvensene usikre. For å bedre forstå hvordan disse systemene påvirkes av klimaendringer trengs referansedata. Her presenteres et øyeblikksstudie av et lite studert, ikke-brepåvirket høyarktisk nedbørfelt (Sarsvatnet, Svalbard). Målet var å utforske de viktigste faktorene som påvirker disse systemene. Vannprøver fra innsjøen og omkringliggende bekker ga et bilde av vannkjemien inkludert sporelementer (Fe, Mn, Al, Ni, As, Co, Cu, Zn, Pb, Cd), hovedioner (Ca^{2+}, HCO_3^-, SO_4^{2-}, Mg^{2+}, Cl^-, Na^+, K^+), pH, konduktivitet, total organisk karbon (TOC) og turbiditet.

Sarsvatnet delte mange kjemiske egenskaper med andre innsjøer på Svalbard, men det ble funnet forhøyede konsentrasjoner av Cu og Zn (henholdsvis 60.74 µg/l og 43.08 µg/l totalt) Ved å bruke en hovedkomponentanalyse (PCA) og sjøsaltkorreksjon ble hovedkildene til de fleste sporelementer og hovedioner vist å være forvitring av berggrunnen og avsetning av sjøsaltaerosoler. Derimot kunne Cd i bekkeprøver kobles til atmosfærisk avsetning, som i dag kan komme av mineralstøv fra nylige isfrie områder på Svalbard. En anrikning av Pb, Mn, Fe, Cu, Zn og Cd i innsjøen sammenlignet med bekkeprøvene kunne muligens bli forklart av avrenning og transport av mineralmateriale fra nedbørfeltet. Denne transporten kan forsterkes av nedbørsepisoder, som dessuten er antatt å øke i fremtiden med et endret klima. Derfor er det et stort behov for mer forskning på variasjoner i vannkjemi, både innad i en sesong og over flere sesonger, for å øke kunnskapen på klimainduserte endringer i Arktis.

Acknowledgments

This is the final work of five amazing years at the Norwegian University of Life Sciences (NMBU). These years have made me realize the importance of environmental sciences, and I will walk out of NMBU with a new driving force to make an impact.

I want to thank my supervisors Thomas Rohrlack and Gunnhild Riise at NMBU for all the help and guidance with my thesis and Eivind Molversmyr for guidance in the lab. I further want to thank the Norwegian Research Council (AFG project number: 322215) for funding the fieldwork to Ny-Ålesund. A big thank you to "Team Mikkelsen" who helped me during my fieldwork and truly made that trip unforgettable. I also want to thank my co-supervisor at the Norwegian University of Science and Technology (NTNU) and The University Centre in Svalbard, Øyvind Mikkelsen, for sharing all your knowledge about Svalbard and helping me organize and execute the fieldwork. The laboratory staff at NTNU also deserves my gratitude for executing my analysis.

Lastly, I want to thank all the people at "Jord" who have made this last year fun with all the laughter and calming walks. I also want to give a special thanks to my brother who helped me proofread and Eirik who has been with me through ups and downs the last four years.

Norwegian University of Life Sciences

Ås, May 2022

Lill Katrin Gorseth

Table of contents

Abbreviations

Al = Aluminum

As = Arsenic

Br^- = Bromide

Br = Bromine

Ca = Calcium

Cd = Cadmium

Cl = Chloride

Co = Cobalt

Cu = Copper

F^- = Fluoride

Fe = Iron

FNU = Formazin Nephelometric Unit

ICP-MS = Inductively coupled plasma mass spectrometry

IC = Ion Chromatography

K = Potassium

LOD = Limit of detection

LRTAP = Long-range transport of atmospheric pollutants

Mg = Magnesium

Mn = Manganese

Na = Sodium

NH_4^+ = Ammonium

Ni = Nickel

NO_2^- = Nitrogen dioxide

NO_3^- = Nitrate

nss = Non-sea-salt

PCA = Principal component analysis

Pb = Lead

PO_4^{3-} = Phosphate

SO_4^{2-} = Sulfate

TN = Total nitrogen

TOC = Total organic carbon

TP = Total phosphorus

Zn = Zinc

List of figures, tables and appendices

1 Introduction

The Svalbard archipelago, a pristine area dominated by glaciers and continuous permafrost, is under pressure from anthropogenic activities (AMAP, 1998). Climate data suggests certain locations on Svalbard are warming up six times faster than the global average (Wawrzyniak & Osuch, 2020). The projected changes in climate may have profound effects on Arctic freshwater systems (Hamilton et al., 2001). However, the consequences are uncertain (CliC/AMAP/IASC, 2016). Nonetheless, these systems are closely linked to climatic processes (White et al., 2007), as well as biogeochemical processes in their catchments (Huser et al., 2022), and changes in these may have an impact on freshwater chemistry.

Svalbard's surface waters cover only about 0.6% of its land area, but include a large diversity of water bodies in terms of e.g., size, hydrological regime, and chemical composition (Birks et al., 2004a; Brittain et al., 2020). Consequently, how they are affected by anthropogenic activities such as climate-induced changes and long-range atmospheric transport of pollutants (LRATP) is highly dependent on individual limnological characteristics. Studies on the chemistry of Svalbard's surface waters are relatively scarce (Brittain et al., 2020; Kozak et al., 2016) and Svalbard's environmental variability calls for individual lake studies.

High Arctic lakes are complex systems and are sensitive even to small-scale changes (Côté et al., 2010). Observations suggest that changes in the physical environment contribute to the fluctuation of certain trace elements in Arctic aquatic organisms (Macdonald et al., 2005). For instance, climatic shifts have been found to alter the trace element flux to Arctic surface waters due to enhanced weathering rates and increased inwash from the catchment (Boyle et al., 2004; Yang et al., 2021). Highly toxic elements, e.g., Cd and Pb, can rapidly move through the trophic levels and potentially magnify (AMAP, 2016; Moiseenko & Gashkina, 2020). Because water is a crucial factor for the fragile Arctic ecosystems, this increased trace element load as a response to a changing climate can have consequences for ecosystem health.

Climatic conditions have a strong influence on High Arctic lakes. Because of the low temperatures on Svalbard, the lakes are only ice-free for a few months during summer (Svenning, 2015). As a result, most lakes are cold-monomictic (Brittain et al., 2020), meaning their water column is mixed at 4°C during summer, but is stratified for the rest of the year (Wetzel, 2001). These temperature gradients in lakes can determine trace element distribution in lakes. This is due to the influence of, e.g., pH and redox conditions on trace element chemistry (AMAP, 1998; Ryan, 2020, p. 248). For instance, a well-mixed lake favors a chemically homogenous water column (Cremer & Wagner, 2003; Semkin et al., 2005). However, due to the logistical difficulties associated with field work on Svalbard (Brittain et al., 2020), there are few studies on vertical trace element distribution in Svalbard lakes. The existing data on trace element composition of lakes is mainly from grab samples from the top layer.

Together with low temperatures, there are also low precipitation rates in the Arctic tundra (Macdonald et al., 2005). However, the precipitation that does fall can play an important role in the scavenging of pollutants and marine aerosols (Macdonald et al., 2000). Because most of the lakes on Svalbard are located near coastal areas, marine aerosols are an important source of sea salt-derived ions (Skjelkvåle et al., 2001). In addition, despite Svalbard's remote location, surface waters are influenced by both naturally and anthropogenically introduced trace elements that travel from lower latitudes (Bindler et al., 2001; Kozak et al., 2016; Law & Stohl, 2007). Through atmospheric transport, contaminants can reach the Arctic within a few days (Polkowska et al., 2011). Long-term air quality data from Ny-Ålesund has shown a significant decrease in the toxic elements Pb (67%), Cd (49%) and As (78%), from 1990 to 2020 (Bohlin-Nizzetto et al., 2021). However, the projected increase in precipitation can make the Arctic an efficient trap for pollutants because of increased scavenging (Macdonald et al., 2005).

Lakes in non-glaciated catchments receive water from precipitation, subsurface flow and the melting of snow and permafrost (Blaen et al., 2014; Rudnicka-Kępa & Zaborska, 2021). The water source can determine the chemical composition, e.g., water from snowmelt can be enriched in pollutants (Dommergue et al., 2010; Kozak et al., 2016) and subsurface water usually has an elevated ion content (Ryan, 2020, p. 100-101). The presence of permafrost generally inhibits extensive subsurface water flow (Hanssen-Bauer et al., 2019), making surface runoff important (Molau, 2016, p. 31). However, a melting active layer, the part of permafrost that thaws during summer, has been found to increase the groundwater influence on stream water chemistry throughout the summer (Blaen et al., 2014; Stutter & Billett, 2003). The active layer in Ny-Ålesund has increased by 20 cm since 2008 (Hanssen-Bauer et al., 2019). These physical changes might increase the subsurface flow and thus increase the hydrological connectivity in catchments (Huser et al., 2022).

The catchment’s features also shape the chemical composition of its surface waters (Kalff, 2002, p. 122). For instance, the geological substratum help determine pH, trace element content and ionic composition through chemical and physical rock weathering (Hall et al., 2002; Kozak et al., 2015; Ruman et al., 2021). As seen in Hjelle (1993), the geology on Svalbard is highly diverse. Consequently, the chemical composition of surface waters may vary greatly (Brittain et al., 2020). Furthermore, because of the harsh climate, High Arctic catchments typically have a sparse vegetation cover (Skjelkvåle et al., 2001). This leaves water bodies low in organic matter and nutrients (Birks et al., 2004b; Kozak et al., 2015; Szumińska et al., 2018), and enhances erosion rates during precipitation events (Berthling & Etzelmüller, 2016). However, this material load is not large enough to influence the clear character of non-glaciated lakes compared to turbid glaciated systems (Brittain et al., 2020).

Temperature has been highlighted as a major external driving force for High Arctic lakes (Birks et al., 2004a). Already, rising temperatures together with altered precipitation patterns have been found to alter natural processes. For instance, Lehmann-Konera et al. (2021) found an increase in the transport of trace elements in a Svalbard river as a response to changing hydrometeorological conditions. Further, studies are reporting the enhanced ionic input to surface waters as a consequence of permafrost thaw (Huser et al., 2022; Roberts et al., 2017; Szumińska et al., 2018). To fully understand how the Arctic freshwater systems are responding to these changes, there is a need for better knowledge of the factors that influence these fragile systems (CliC/AMAP/IASC, 2016).

This snapshot study explores the water chemistry of a poorly investigated High Arctic lake at the end of a summer season to increase the knowledge on factors affecting these systems. The studied catchment (Lake Sarsvatnet) is located near Ny-Ålesund on Svalbard, a pristine area under pressure from climate change. Boyle et al. (2004) previously emphasized the impact of climatic shifts on the temporal changes in trace element distribution in the sediments of Lake Sarsvatnet. There are no known trace element data from these surface waters. Thus, this study will function as a baseline for future research. Moreover, this research will increase the relatively scarce existing data on trace element composition of High Arctic surface waters at a time when there is a great need for baseline condition data (Côté et al., 2010).

The main objective of this study is to explore the distribution and identify sources of trace elements (Fe, Mn, Al, Ni, As, Co, Cu, Zn, Pb and Cd) and major ions in Lake Sarsvatnet with its surrounding inlet and outlet streams. To investigate this, lake and stream samples collected in August 2021 are used to explore the vertical distribution of trace elements in the lake's water column as well as analyze the lake chemistry against stream chemistry. The following research question is addressed:

What are the main factors influencing the trace element and major ion composition of the Lake Sarsvatnet catchment at the end of summer?

2 Materials and methods

2.1 Study area

The sampling for this study was conducted around the Ossian Sars Mountain (364 m a.s.l.), located in the High Arctic on the west coast of Svalbard's largest island, Spitsbergen (Figure 1). The area is surrounded by the glacier Kongsbreen in the innermost part of Kongsfjorden, approximately 12 km west of the research station, Ny-Ålesund. Ossian Sars is protected through a nature reserve due to the presence of rare plant species and to protect an untouched area (Forskrift om Ossian Sars naturreservat, 2003). In 2021, the mean annual temperature in the area was -2,9°C and the annual precipitation was 453 mm at the nearest meteorological station in Ny-Ålesund (Norsk Klimaservicesenter, n.d.).

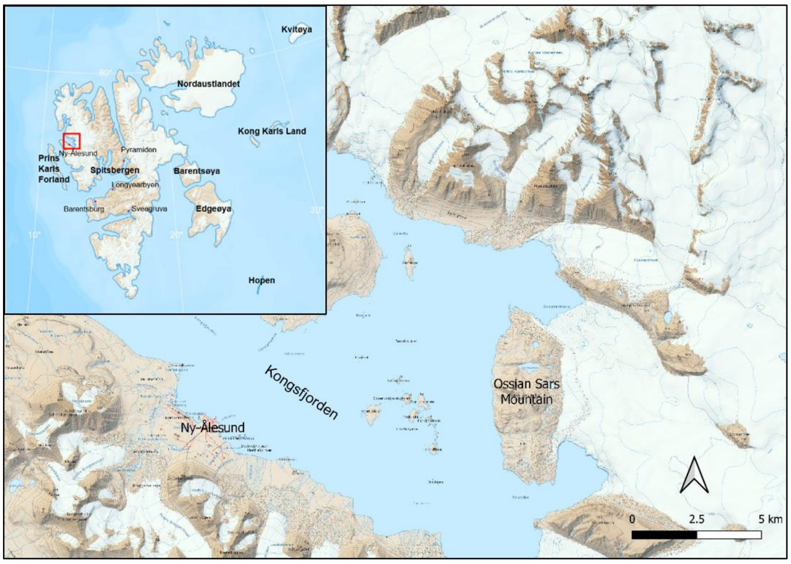

Figure 1: Map of Svalbard (upper left) and the Kongsfjorden area. Data set from: Norwegian Polar Institute (2013).

There are several small lakes and streams around the mountain, but this study focuses on Lake Sarsvatnet (100 m a.s.l) with its surrounding inlet and outlet streams. Lake Sarsvatnet (Figure 2) has an area of 0.22 km^2, a maximum depth of 24 meters (Figure 3) and a roughly estimated water residence time of around 4 years (calculation shown in Appendix A). As with many other non-glaciated lakes on Svalbard, Lake Sarsvatnet is clear and ultraoligotrophic (Lindström & Leskinen, 2002), with a Secchi-depth of approximately 19 m (Birks et al., 2004b). Furthermore, Lake Sarsvatnet has a high pH (~8) (Birks et al., 2004b) and a sedimentation rate of 0.027 cm/year (Appleby, 2004). Because of the climate on Svalbard, the lake is only ice-free for a couple of months during summer (Laybourn-Parry & Marshall, 2003).

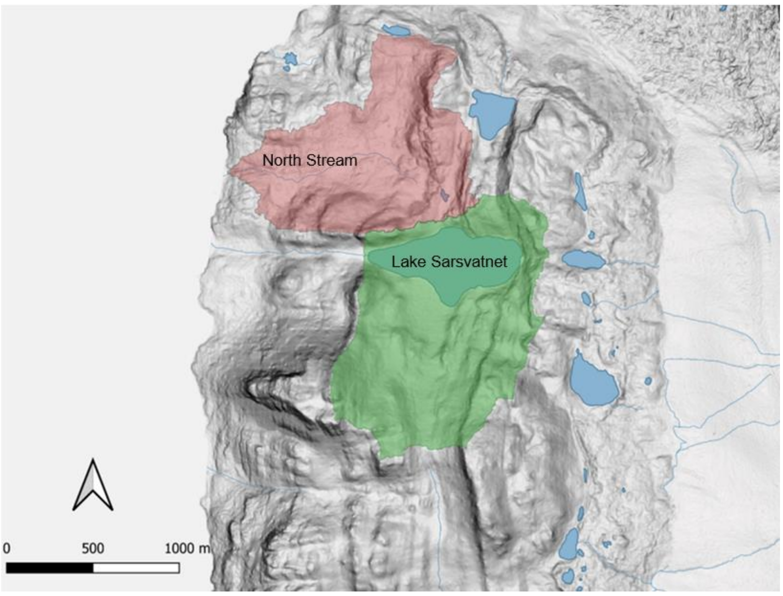

Figure 2: Topographic map of the two catchments included in this study. Lake Sarsvatnet's catchment is colored in green and the north stream's catchment is in red. Data set derived from: Norwegian Polar Institute (2014a) and Norwegian Polar Institute (2014b).

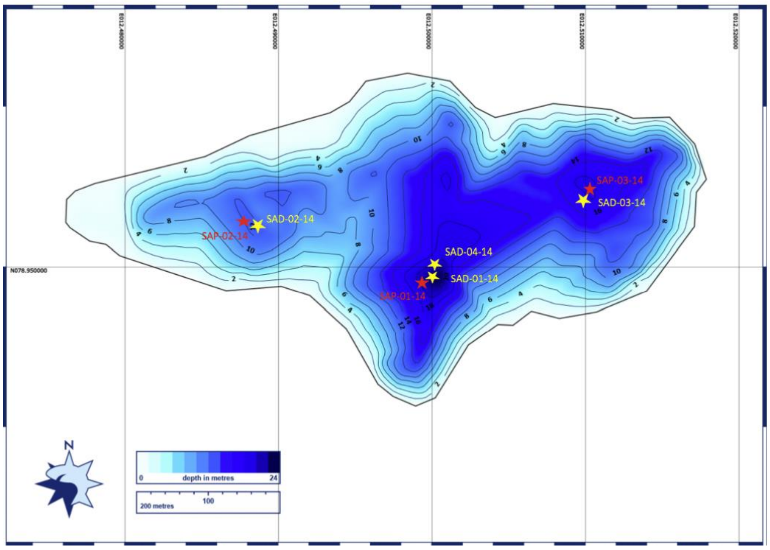

Figure 3: Bathymetric map of Lake Sarsvatnet. Figure derived from Bjerkås (2019).

Lake Sarsvatnet's catchment (Figure 2) is approximately 1,3 km^2 (Bjerkås, 2019) and is sparsely vegetated (Appendix B). Furthermore, solifluction has previously been observed in the catchment (Birks et al., 2004b). There are no glaciers in the catchment and the lake's input of water is therefore likely from snowmelt and precipitation. Because these inputs vary throughout the season, the inlet streams are believed to have a variable water discharge. At the end of summer, the branched inlet streams on the south side drain through a vegetated area (Appendix C). On the west side of the lake, the outlet stream drains into Kongsfjorden. Because the outlet stream originates from a lake, the water discharge is likely more stable throughout the summer (Brittain et al., 2020).

To increase data on stream water chemistry that resembled the inlet streams, sampling was conducted in a stream north of Lake Sarsvatnet's outlet stream. This stream is hereafter referred to as the "north stream" (Figure 2), and is a small stream that drains directly into the fjord. It receives water from the surrounding catchment, with precipitation and snowmelt as the main sources. This non-glaciated catchment is approximately 1.1 km^2 and is dominated by slightly more vegetation than Lake Sarsvatnet's catchment (Appendix B).

The geology at Ossian Sars is dominated by mica schist, quartzite, and phyllite (Bjerkås, 2019) close to the fjord (Signehamna formation), with elements of marble and dolomite (Generalfjella formation) running north-south (Figure 4)(Dallmann, 2015; Hjelle, 1993; Hjelle et al., 1999). Further east, close to the glacier, the area is dominated by marble and dolomite. Large parts of the area are covered with glacial till with some elements of weathered bedrock and landslide material (Bjerkås, 2019).

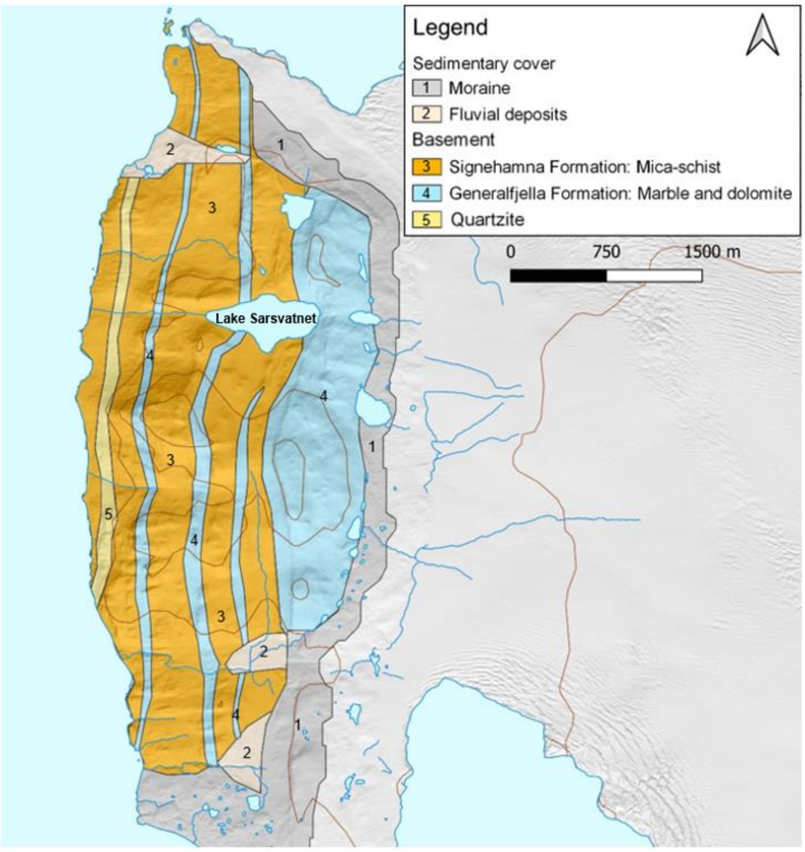

Figure 4: Geological map of Ossian Sars including sedimentary cover and basement. The map is modified from Hjelle et al. (1999) and Bjerkås (2019). Data set from Norwegian Polar Institute (2016a).

2.2 Fieldwork

Fieldwork was conducted from the 18th to 19th of August 2021 with the help of co-supervisor Øyvind Mikkelsen and students at the Norwegian University of Life Sciences (NMBU) and the Norwegian University of Science and Technology (NTNU)(Appendix C). Water samples from inlet streams, Lake Sarsvatnet, outlet stream and the north stream were obtained, resulting in 20 sampling points (Figure 5)(Appendix D).

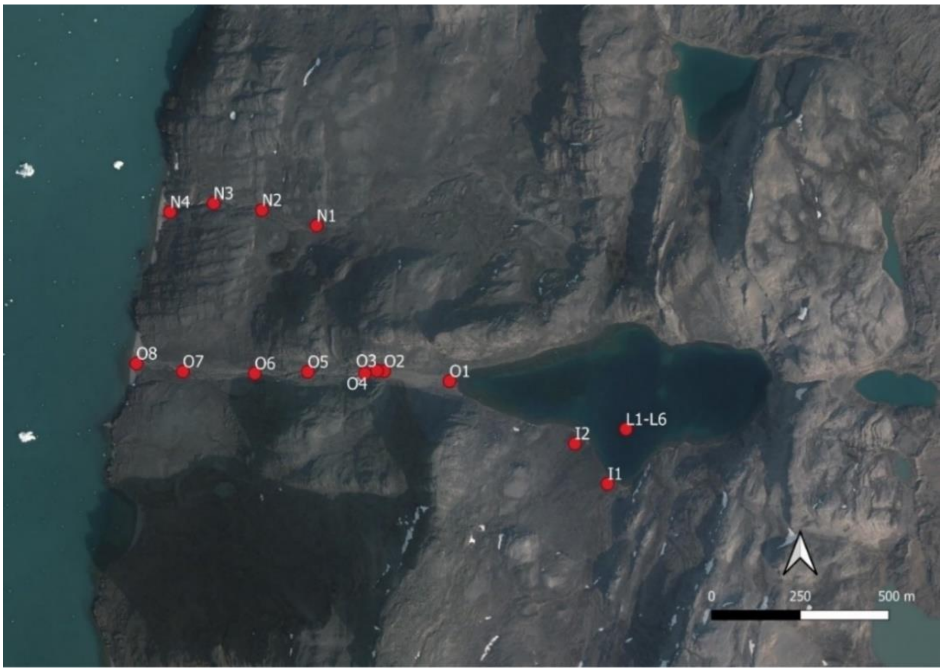

Figure 5: Satellite map of the sampling locations in inlet streams (I1 and I2, lake (L1-L6), outlet stream (O1-O8) and the north stream (N1-N4) at Ossian Sars. Data set from Norwegian Polar Institute (2016b).

2.2.1 Lake Sarsvatnet

Water samples from Lake Sarsvatnet were collected by boat following Norwegian Standard NS-ISO-5667-4. Near the estimated deepest point in the lake, six depths were chosen in-field to show the distribution of elements in the water column: 0.5 m (L1), 3.0 m (L2), 7.0 m (L3), 11.0 m (L4), 15.0 m (L5) and 19.0 m (L6) (Figure 6). To obtain the water samples, a plastic water collector was used (Figure 6). Water from each depth was filled up in 3x50mL + 1x15 mL tubes and temperatures were measured using a digital thermometer (accuracy of ± 0.5°C).

Figure 6: Left: Water sampling from various depths in Lake Sarsvatnet. Photo: Sunniva Kvamme. Right: Water collector used to obtain water samples in the lake. Photo: Lill Katrin Gorseth

2.2.2 Streams

Water samples were also collected at seven locations in the outlet stream (O1 – O7, Figure 5) and four locations in the north stream (N1 – N4, Figure 5). The idea was to obtain multiple water samples in several of Lake Sarsvatnet's inlet streams. However, this was proven difficult due to low water discharge. Hence, only one sample in each of the two identified inlet streams was obtained (I1 and I2, Figure 5). The water samples were filled in 4x50 mL tubes following Norwegian Standard NS-ISO 5667-6.

2.2.3 In-field preparation of samples

Immediately after arriving back in Ny-Ålesund, water samples were handled for further analysis. For all water samples, 2x10 mL was transferred into separate tubes for analysis by ICP-MS. One of the 10mL-samples from each location was filtered with a single-use syringe and a 0.45 µm filter. ICP-MS samples were then acidified with ultra-pure concentrated (65%) HNO_3. All water samples were immediately put in the fridge at 4°C and kept cold until travel back to NMBU or NTNU for further analysis.

2.3 Sample analysis

At sampling locations O1 and O6, fewer tubes with water samples were obtained. Consequently, not all analyses were conducted on these samples. All samples except sample

O1 and O6 were analyzed for total organic carbon (TOC), total phosphorus (TP), total nitrogen (TN), ammonium-nitrogen (NH_4-N), pH, conductivity, and turbidity at NMBU. The analyses done at NMBU were executed by the MSc student with guidance from lab-personnel. Furthermore, all samples except for sample O1 were analyzed for major anions at NTNU. Both filtered and unfiltered samples from all locations were analyzed by ICP-MS at NTNU. The analyses done at NTNU were executed by lab-personnel.

2.3.1 Laboratory analysis

Turbidity, conductivity, and pH

Turbidity, conductivity, and pH were analyzed in-lab using the same unfiltered water sample in the following order. Turbidity measures the content of suspended particles in water and was conducted with a HACH 2100AN IS Turbidimeter following Norwegian Standard NS-ISO 7027-2. Turbidity is expressed in Formazin Nephelopmetric Unit (FNU).

Conductivity is a measurement of the ability of the water to conduct electricity, related to the content of suspended ions. It was measured with a 914 pH/Conductometer from Metrohm following Norwegian Standard NS-ISO 7888. Conductivity is expressed in µS/cm. Lastly, pH was measured following Norwegian Standard NS-EN ISO 10523 using a PHM210 Standard pH meter from MeterLab. The instrument was calibrated with pH 4 and pH 7 before use.

Total organic carbon

TOC is used as a measure of the total amount of organic matter present in the water sample. To determine TOC, unfiltered water samples were analyzed using a Shimadzu Total Organic Carbon Analyzer (TOC-VCPH) with a detection limit of 0.2 mg/l. The procedure followed Norwegian Standard NS-EN 1484.

Total nitrogen

Unfiltered water samples were added an oxidizing agent, potassium persulfate in a basic solution, to oxidize all nitrogen to nitrate (NO_3^-). All samples were put into an autoclave for 30 minutes. Lastly, the samples were diluted 10.5 times with distilled water. Total nitrogen was analyzed following Norwegian Standard NS 4743 using a Lachat IC5000 Ion Chromatography with a detection limit of 0.02 mg/l.

Total phosphorus

A strong oxidizing agent, potassium peroxydisulfate was added to unfiltered water samples to oxidize all phosphorus to orthophosphate. After autoclaving, ascorbic acid and molybdate were added to react with the orthophosphate and form a blue complex that was measured by a spectrophotometer after 20 minutes. This was done with a Hitachi UH5300 Spectrophotometer at 880 nm with a 2 cm cuvette. The detection limit for TP is 5 μg/l and the procedure followed Norwegian Standard NS-EN ISO 6878.

Ions

To measure NH_4-N, unfiltered samples were added hypochlorite and salicylate. After at an hour, the samples were read of with a Hitachi UH5300 spectrophotometer at 655 nm using a 1 cm cuvette. The detection limit for NH_4-N is 20 μg/l. The procedure followed a modified version of NS 4746 by Digernes (2004). For the major anion analysis, the following ions were analyzed: sulfate (SO_4^{2-}), NO_3^-, nitrogen dioxide (NO_2^-), fluoride (F^-), chloride (Cl^-), phosphate (PO_4^{3-}), bromide (Br^-) using the 940 Professional IC Vario Ion Chromatograph. Prior to analysis, the samples were filtered using a single-use syringe and a 0.45 μm filter. The detection limit is 0.2 mg/l.

ICP-MS

Inductively coupled plasma mass spectrometry (ICP-MS) was used to analyze both filtered and unfiltered water samples using the Agilent 8800 Tripple Quadrupole ICP-MS. The ICP-MS instrument turns the water sample into aerosols that are led into a plasma measuring 6000-8000°C. This ionizes the sample components, and the gas is further separated into ions before measured with a detector.

2.3.2 Analytical errors

Field blanks could have captured any in-field contamination, but due to lack of distilled water, only lab blanks were used. In addition, because of a defect in the pipette during the TP analysis, sample O5 was contaminated and consequently left out of the results. Furthermore, the pH-probe was calibrated with standards of pH 4 and 7 instead of the ideal calibration using standards of 7 and 9 which were inside the pH range of the samples. Lastly, there were troubles with the sensibility for PO_4^{3-} on the Ion Chromatography (IC) during the analysis, meaning PO_4^{3-} could have been present at low concentrations without being detected.

2.4 Meteorological data

Meteorological data was gathered using the website seklima.met.no (Norsk Klimaservicesenter, n.d.). The closest weather station is in Ny-Ålesund (78.94970°N 12.49878°E) at 10 m altitude, so some deviation from the weather at Ossian Sars might have occurred due to location and altitude differences.

2.5 Data treatment and analysis

Primary data was organized and handled in Microsoft Office Excel 365 (Version 2203). Filtered samples were used to obtain the dissolved fraction. The particulate fraction was calculated by subtracting filtered samples from unfiltered samples. For some of the elements, negative values for the particulate fraction occurred. These were set to zero in figures. Statistical analyses, Principal component analysis (PCA) and Spearman correlation test, were conducted using R-studio (Version 4.1.2).

2.5.1 Principal component analysis

Principal component analysis (PCA) can be used to identify similar patterns in a large data set. A PCA was performed on filtered stream samples. Biplots were made using the first two principal components. Missing data (N/A) were imputed using the "missMDA"-package in R-studio. Data values under the detection limit were added into the data as half the values of the associated detection limits (LOD). Prior to analysis, the data was standardized and scaled. The variables included in the PCA were Cd, Zn, Ni, As, Cu, Co, Al, Fe and Mn, in addition to pH, conductivity, TOC, Ca, SO_4^{2-}, Mg and K. Furthermore, Br, Na and Cl^- were included as tracers for atmospheric deposition.

2.5.2 Spearman correlation test

To investigate any relationships between the variables tested, a Spearman correlation test was executed. A Spearman correlation test can be used for non-normally distributed data. Spearman's correlation coefficients (ρ) were calculated for the same data as the PCA. The correlation coefficients between two variables are values between 1 and -1, where 1 indicates a perfect positive relationship and -1 indicates a perfect negative relationship.

2.5.3 Estimation of non-sea-salt ion concentrations

To estimate the influence of marine aerosols on the ion concentrations, non-sea-salt (nss) ion contributions were calculated using Cl^- concentrations. This method followed Szumińska et al. (2018) and ion/Cl^- ratios used are listed in Krawczyk and Pettersson (2007). The following equation was used:

$$\textit{nss ion concentration} = \textit{total ion concentration} - \textit{ratio} \times Cl^- \textit{ concentration}$$

3 Results

This chapter includes selected results from investigated surface waters at Ossian Sars. First, meteorological data from 2021 are presented, followed by selected chemical and physical water parameters. Following this, hydrochemical data is shown where trace elements and major ions are treated separately. Additional results excluded from this chapter are listed in Appendix E, Appendix F,Appendix G, Appendix H and Appendix I.

3.1 Meteorological background

To get an overview of the meteorological situation from January to August in 2021 and explore if this was a representative year compared to the 1991-2020-normal, both average and normal temperature and precipitation values are listed in Table 1. Meteorological data showed that the winter and spring in 2021 was warmer and dryer than normal. Further, summer temperatures were more in accordance with the average temperatures, where mean temperatures (T) in June (T=2.6°C) and July (T=5.5°C) were slightly colder and August was slightly warmer (T=5.2°C) than normal. From the total monthly precipitation data (P), July (P=14 mm) was considerably dryer as it rained 18.1 mm less than the monthly normal, and August was slightly wetter (P=32.4mm).

Table 1: Meteorological data from Ny-Ålesund including monthly average temperature (°C), monthly normal (1991-2020) temperature (°C), monthly average precipitation (mm) and deviation from precipitation normal (1991-2020) (mm) from January-August 2021.

Month (2021)	Average temperature (°C)	Temperature deviation from monthly normal 1991-2020 (°C)	Monthly precipitation (mm)	Precipitation deviation from monthly normal 1991-2020 (mm)
January	-7.9	2.4	60.8	5.1
February	-6.1	5.1	31.4	-11.3
March	-9.1	2.5	38.4	-2.5
April	-6.8	1.9	23	-2.1
May	-3.8	-1.4	13.1	-6.6
June	2.6	-0.2	19.6	5.6
July	5.5	-0.3	14.0	-18.1
August	5.2	0.6	32.4	-5.4

In the weeks prior to sampling (01.08.2021 – 19.08.2021), the total precipitation rate was 20.8 mm (Figure 7). The last precipitation event before sampling occurred from August 12th to 13th with daily precipitation rates of 2.6 mm and 5.8 mm, respectively. Before this, another precipitation event lasting for four days ended on August 8th. The daily mean wind intensity in the same period ranged from 0.9 – 8.5 m/s. In the week prior to sampling (12.08.2021 – 18.08.2021), the wind intensity was 0.9 – 3.8 m/s.

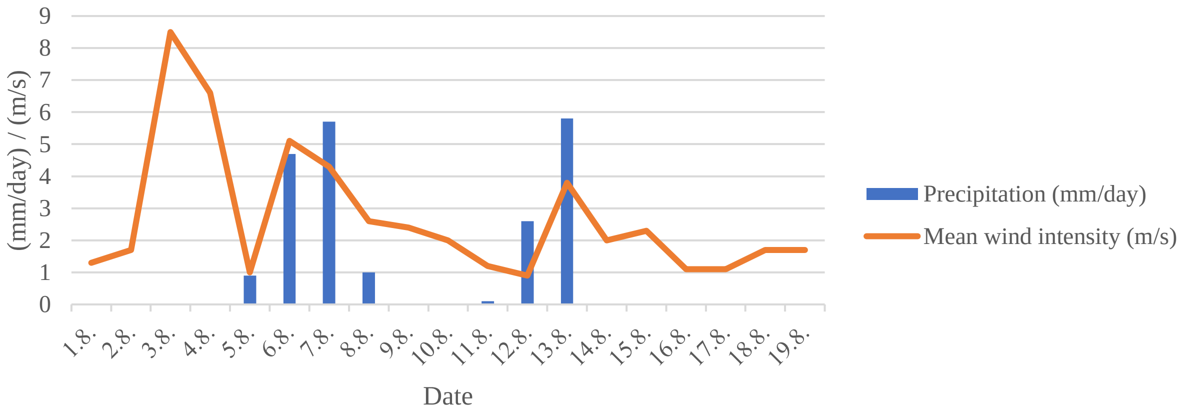

Figure 7: Daily precipitation (mm/day) and daily mean wind intensity (m/s) from 01.08.21 - 19.08.21 in Ny-Ålesund.

3.2 Selected chemical and physical parameters

TOC content ranged from 1.6 – 2.1 mg/l in lake samples and from 0.8 – 3.2 mg/l in stream samples (Table 2). The north stream showed higher concentrations compared to the outlet stream but was similar to the inlet streams and the lake. The turbidity values were all under 1.4 FNU.

These surface waters showed a neutral to alkaline character. The pH-values in all water samples were similar and ranged from 7.7 (L6) to 8.1 (N1) (Table 2). Conductivity showed a more diverse distribution, where inlet streams and the north stream had higher values than the lake and outlet stream. The north stream had values reaching almost 300 µS/cm, whereas lake conductivity was well below 200 µS/cm.

Table 2: Selected chemical and physical factors including pH, turbidity (FNU), conductivity (µS/cm) and total organic carbon (TOC, mg/l) in water samples from Ossian Sars.

Category	Sample	pH	Turbidity [FNU]	Conductivity [µS/cm]	TOC [mg/l]
Inlet streams	**I1**	7.8	0.6	248	3.2
	I2	8.1	0.3	245	1.2
Lake	**L1 (0.5 m)**	8.0	0.5	186	1.8
	L2 (3 m)	8.0	0.4	187	1.9
	L3 (7 m)	8.0	0.4	190	1.8
	L4 (11 m)	7.9	0.7	193	1.6
	L5 (15 m)	7.8	0.9	188	2.1
	L6 (19 m)	7.7	1.4	198	1.6
Outlet stream	**O1**	N/A	N/A	N/A	N/A
	O2	7.9	0.2	187	1.1
	O3	7.8	0.2	197	0.9
	O4	8.0	0.5	202	1.1
	O5	8.0	0.4	213	0.9
	O6	N/A	N/A	N/A	N/A
	O7	8.0	0.3	213	0.8
	O8	8.0	0.5	216	0.9
North Stream	**N1**	8.1	0.3	295	1.5
	N2	8.0	0.3	291	1.5
	N3	8.0	0.4	296	1.3
	N4	8.1	0.2	298	1.9

The lake temperature measurements in-field (August 18th) are shown in Figure 8. There was a temperature gradient in the water column with an approximately 3°C difference from the top warmer layers compared to the bottom colder layers.

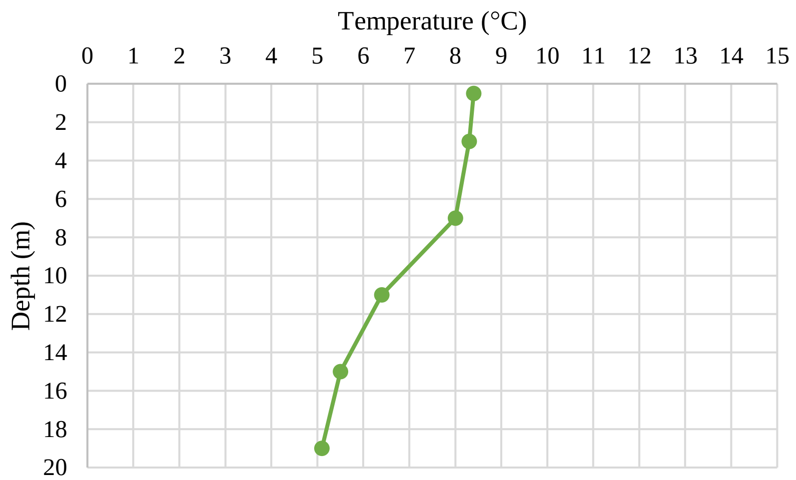

Figure 8: Temperature data from a vertical profile in Lake Sarsvatnet on August 18th, 2021.

3.3 Distribution of selected trace elements

In this section, selected trace elements (Fe, Mn, Al, Ni, As, Co, Cu, Zn and Pb) are presented to show their distribution across the lake and streams. Elements showing a similar distribution are treated together. To highlight if the elements appear in the dissolved or particulate phase, they are shown together, making up the total concentration.

3.3.1 Fe, Mn and Al

Fe, Mn and Al showed a diverse distribution across the sampling locations and high particulate concentrations in the bottom lake sample (L6). Fe appeared mostly in the particulate phase and had an uneven distribution ranging from 0.9 – 309.1 µg/l (Figure 9). The dissolved fraction was more even, ranging from 0.42 – 8.04 µg/l. Overall, the highest concentrations of Fe were found in Lake Sarsvatnet.

Stream concentrations of Mn were lower than the lake samples (Figure 10). Similar to Fe, most Mn was found in the particulate phase across most sampling locations. Mn showed a similar distribution as Fe, with highest concentrations in the lake. Dissolved Mn ranged from <LOD – 10.06 µg/l and particulate Mn ranged from 0 – 76.67 µg/l.

Al showed a somewhat different distribution than Fe and Mn with a more even distribution across lake and stream samples (Figure 11). Further, a higher fraction of Al appeared in the dissolved phase compared to Fe and Mn. Dissolved Al ranged from 1.10 – 3.61 µg/l and particulate Al ranged from 0 – 149.08 µg/l. Sample L6 had a substantially higher value than the other samples and was left out of the figure to show the variation across sampling points.

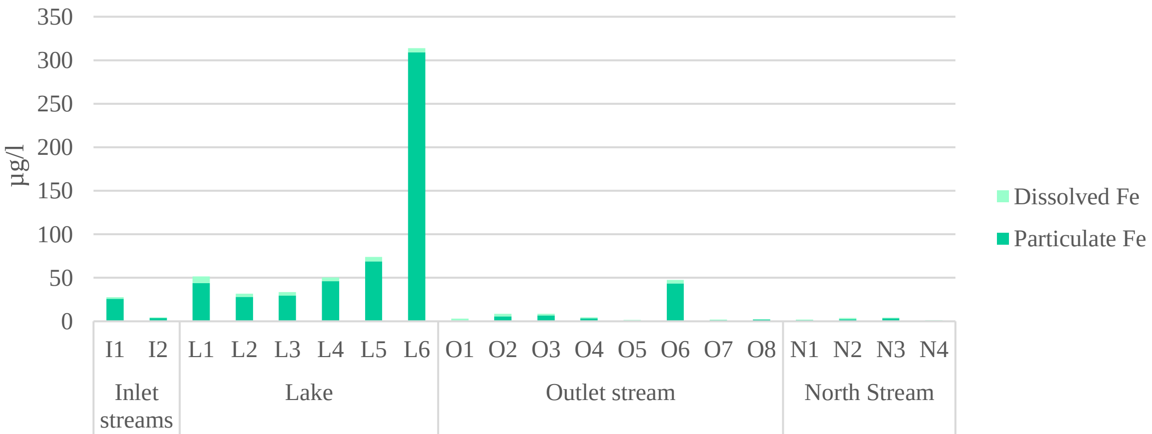

Figure 9: Iron (Fe) concentrations (µg/l) in the studied surface waters. The dissolved and particulate fraction is shown, making up the total concentration.

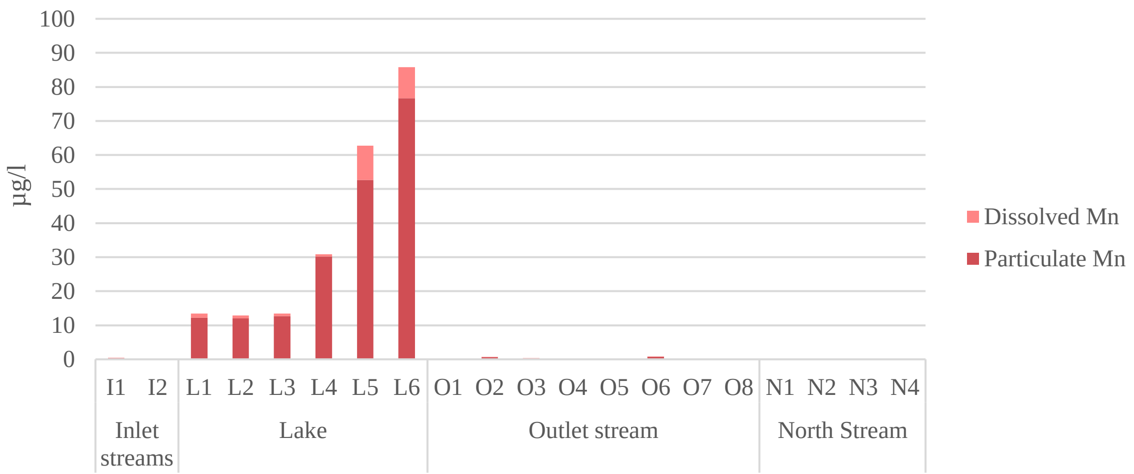

Figure 10: Manganese (Mn) concentrations (µg/l) in the studied surface waters. The dissolved and particulate fraction is shown, making up the total concentration.

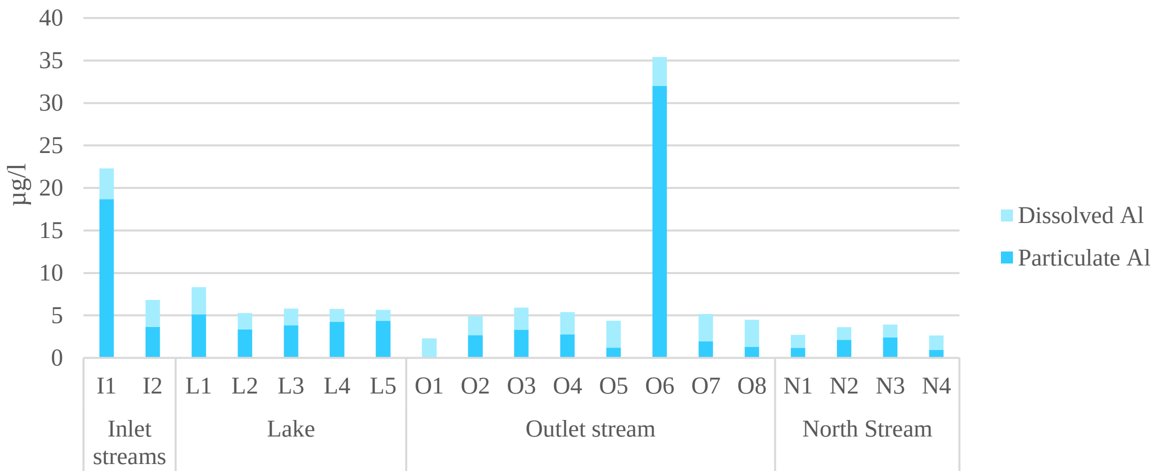

Figure 11: Aluminium (Al) concentrations (µg/l) in the studied surface waters. The dissolved and particulate fraction is shown, making up the total concentration. Because Sample L6 had a substantially higher value than other samples, it was left out of the figure to show the variation across sampling sites.

3.3.2 Ni, As and Co

Ni, As and Co revealed a similar distribution across the sampling locations with an even distribution across the streams and the lake. Ni appeared mostly in the dissolved phase, where dissolved concentrations ranged from 0.16 – 0.40 µg/l and particulate ranged from 0 – 0.18 µg/l (Figure 12). This was also true for As, where dissolved concentrations ranged from 0.07 – 0.19 µg/l and particulate concentrations ranged from 0 – 0.03 µg/l (Figure 13). Dissolved Co concentrations ranged from 0.01 – 0.04 µg/l and particulate from 0 – 0.14 µg/l (Figure 14). Lake sample L6 stood out due to the higher content of particulate Co, which was also true for Ni and As, but to a lesser degree.

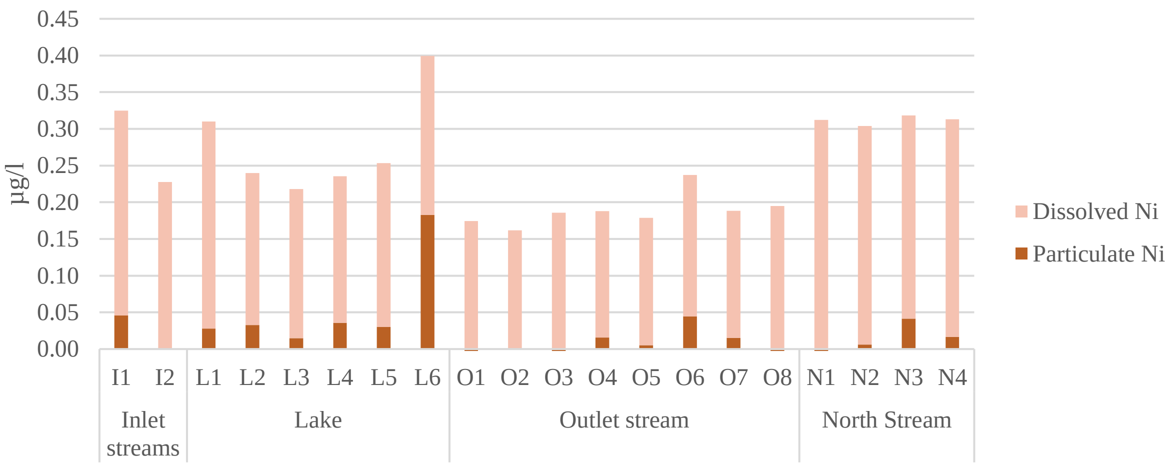

Figure 12: Nickel (Ni) concentrations (µg/l) in the studied surface waters. The dissolved and particulate fraction is shown, making up the total concentration.

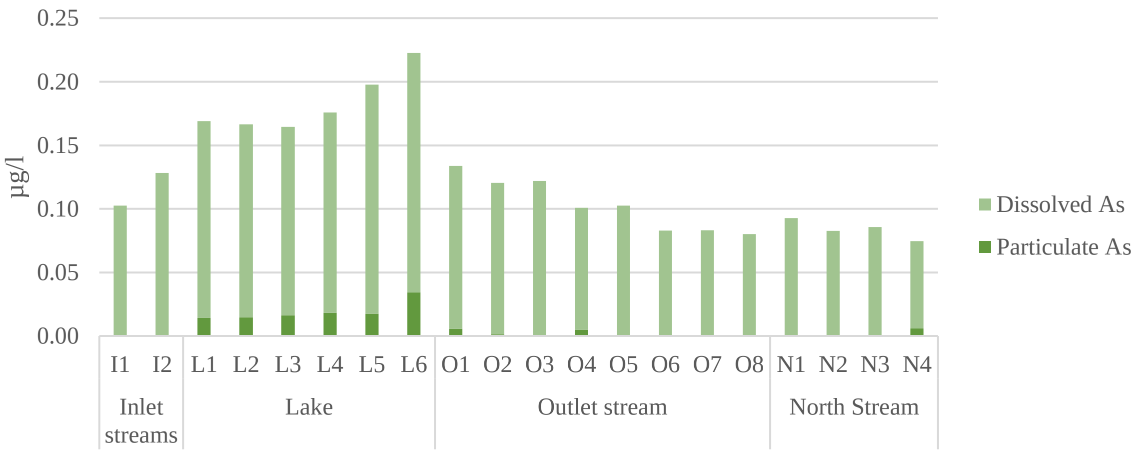

Figure 13: Arsenic (As) concentrations (µg/l) in the studied surface waters. The dissolved and particulate fraction is shown, making up the total concentration.

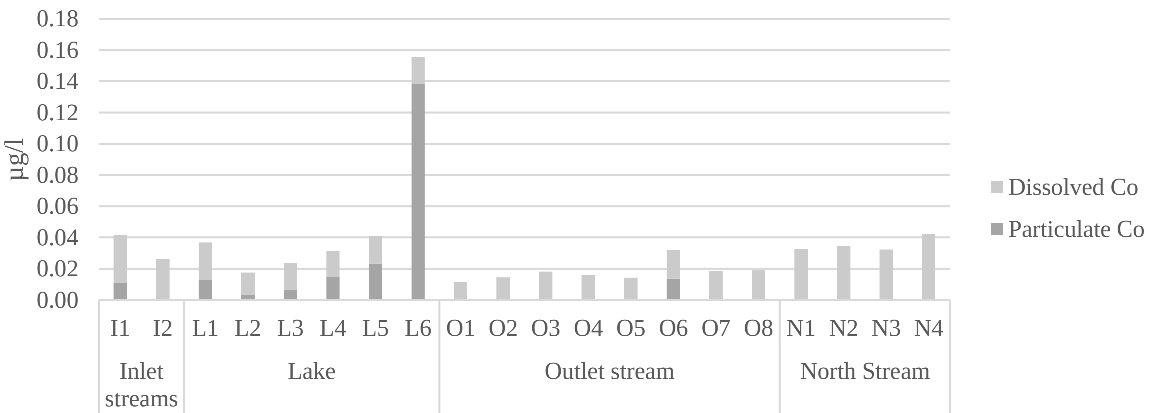

Figure 14: Cobalt (Co) concentrations (µg/l) in the studied surface waters. The dissolved and particulate fraction is shown, making up the total concentration.

3.3.3 Cu, Zn, Pb and Cd

Cu, Zn, Pb and Cd showed a similar distribution across the sampling locations. The most apparent observation was that these trace elements showed higher concentrations in the lake compared to the streams. Dissolved Cu concentrations ranged from 0.27 – 17.07 µg/l and particulate from 0 – 43.67 µg/l (Figure 15). Dissolved Zn ranged from 0.56 – 27.17 µg/l and particulate from 0 – 15.91 µg/l (Figure 16). Pb was only detected in lake samples, where dissolved concentrations ranged from 0.02 – 0.55 µg/l and particulate from 0.92 – 2.14 µg/l (Figure 17) Lastly, dissolved Cd concentrations ranged from 0.001 – 0.011 µg/l and particulate from 0 – 0.035 µg/l (Figure 18). Interestingly, they all showed a higher concentration of both dissolved and particulate fractions in the top layer of the lake compared to the rest of the water column.

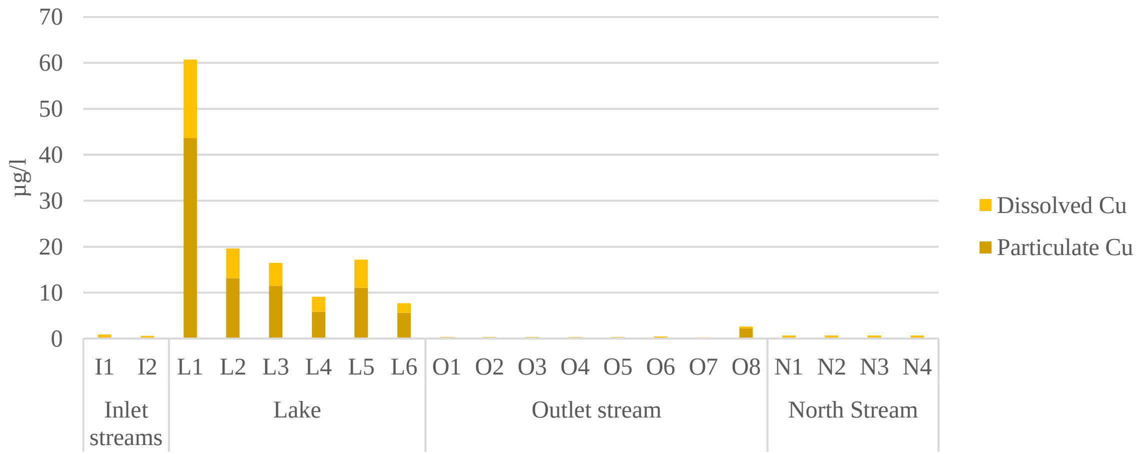

Figure 15: Copper (Cu) concentrations (µg/l) in the studied surface waters. The dissolved and particulate fraction is shown, making up the total concentration.

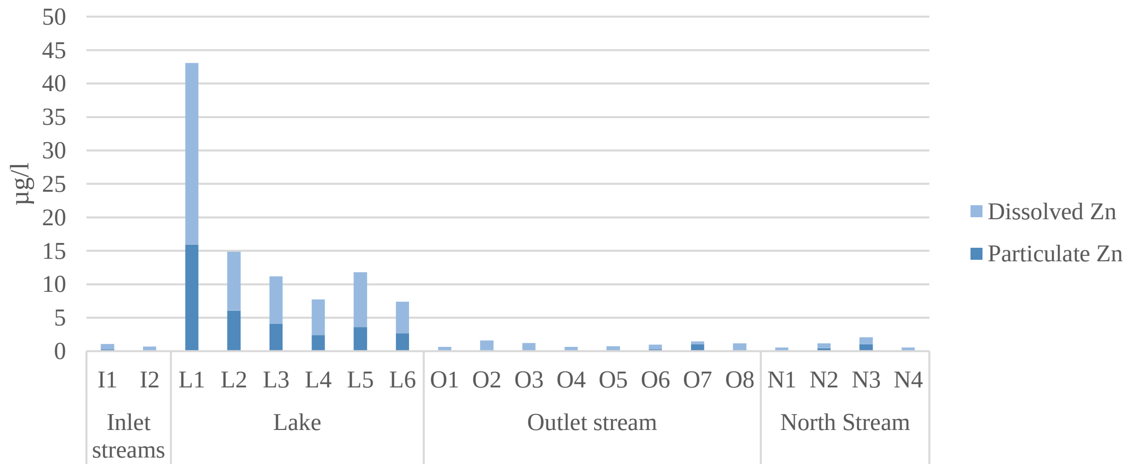

Figure 16: Zinc (Zn) concentrations (µg/l) in the studied surface waters. The dissolved and particulate fraction is shown, making up the total concentration.

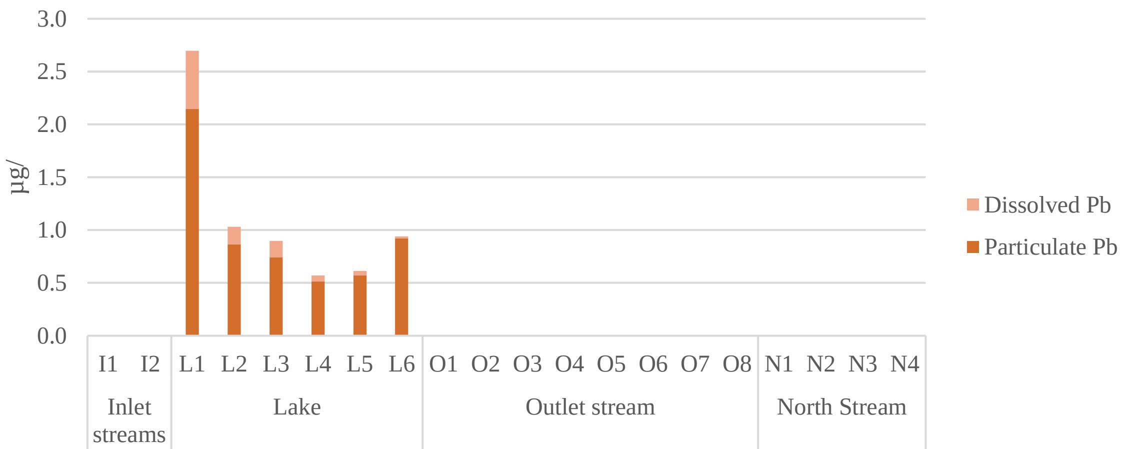

Figure 17: Lead (Pb) concentrations (μg/l) in the studied surface waters. The dissolved and particulate fraction is shown, making up the total concentration.

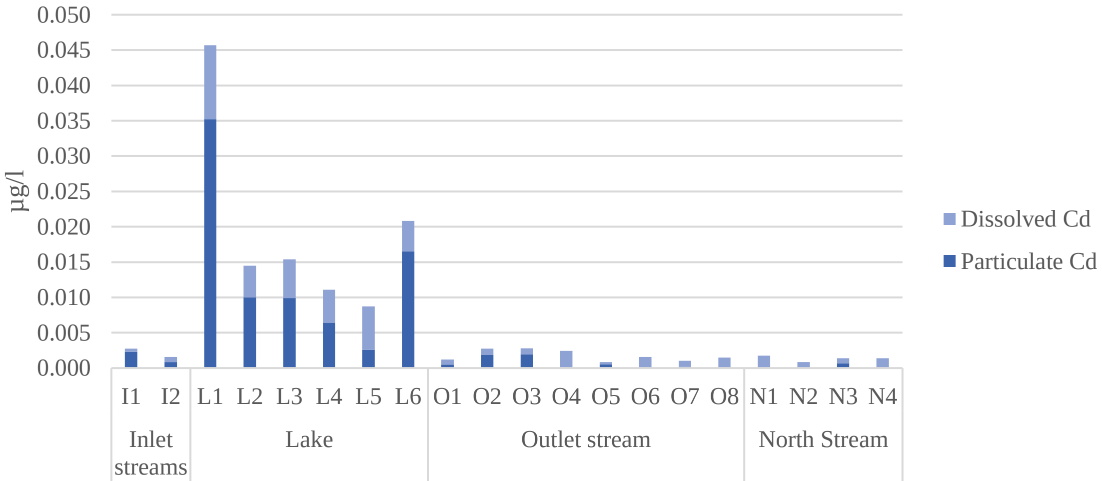

Figure 18: Cadmium (Cd) concentrations (μg/l) in the studied surface waters. The dissolved and particulate fraction is shown, making up the total concentration.

3.4 Distribution of major ions

The major ion composition in all dissolved water samples is shown in Figure 19. Because organic matter content was low, it is assumed that most ions were on dissolved form. Thus, the dissolved values are presented as ions. HCO_3^- was not measured in-lab but estimated by subtracting the major anions from the major cations, where the difference was used as a proxy for alkalinity. Sample O1 was left out of the figure because of missing IC data.

In all locations, Ca^{2+} and HCO_3^- were the main ions followed by SO_4^{2-}, Mg^{2+}, Cl^-, Na^+ and K^+. Highest concentrations of major ions were found in the north stream and the inlet streams, coinciding with higher conductivity values in these samples. The north stream had a higher overall content of HCO_3^-, SO_4^{2-}, Ca^{2+} and Mg^{2+} than the other sampling locations.

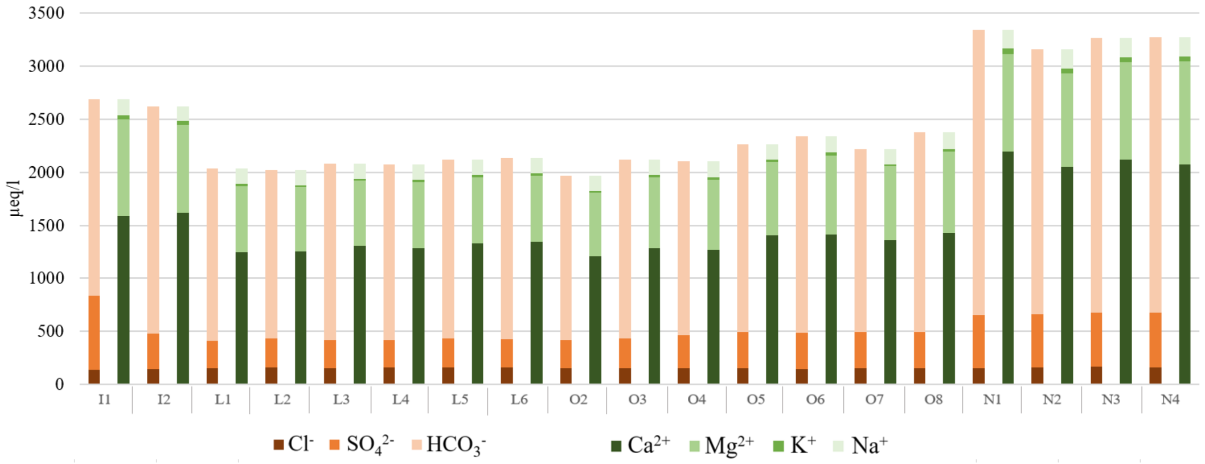

Figure 19: Major ion composition (Cl^-, SO_4^{2-}, HCO_3^-, Ca^+, Mg^{2+}, K^+, Na^+) of water samples expressed in µeq/l. O1 is not included because Ion Chromatography data on Cl^- and SO_4^{2-} was missing. HCO_3^- was not measured in-lab, but calculated by subtracting the anions from the cations. The difference was used as a proxy for alkalinity.

3.5 Statistics

A PCA biplot for PC1 and PC2 is shown in Figure 20, explaining 51% and 20% of the variance, respectively. From this, three groupings were identified. One group consisted of Al, Fe and Zn that correlated negatively with PC1. Another grouping included Cd, Br, Cl^- and pH which correlated positively with PC2. A third grouping, Ca, Co, Na, K, Ni, Mg and conductivity (Cond in figure), correlated positively with PC1. In addition, Cu and SO_4^{2-} grouped together and correlated positively with PC1. TOC and Mn did not show a clear grouping with the other variables.

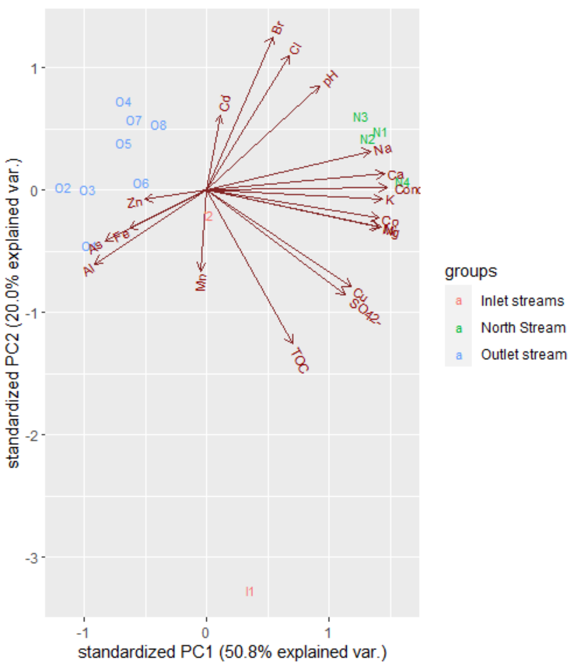

Figure 20: PCA biplot including the variables pH, conductivity (Cond), total organic matter (TOC), Br, Cl^-, Na, Ca, K, Mg, Ni, Cu, SO_4^{2-}, Mn, As, Fe, Al, As, Zn and Cd. On the right side, Ni and Mg are on top of each other under Co.

4 Discussions

In the following sections, factors influencing the observed chemical composition of Lake Sarsvatnet system are discussed, including metrological conditions, atmospheric deposition, geochemical factors and the influence of subsurface flow. Lastly, this study attempts to define Lake Sarsvatnet's characteristics and compare the chemical features of this lake system to other lakes on Svalbard.

4.1 Influence of meteorological conditions on trace element distribution

Pb, Cu, Zn, Cd, Mn and Fe showed markedly higher concentrations of both dissolved and particulate fractions in the lake compared to the streams (Figure 9, Figure 10, Figure 15, Figure 16, Figure 17, Figure 18). Although there could be several factors contributing to this observation, one explanation may be the input of a catchment derived material as a response to precipitation events as proposed by Boyle et al. (2004). The authors argued that precipitation events influenced the temporal trace element distribution in the sediments of Lake Sarsvatnet. Furthermore, the authors suggested one of the main sediment inputs to be a catchment derived, minerogenic material, enriched in organic matter, Mn, Fe, Cu, Pb, Zn, and possibly other trace elements. Lewis et al. (2012) also stated the importance of precipitation in the flux of catchment material to surface waters. Due to the scarce vegetation cover in Lake Sarsvatnet's catchment, erosion is more likely to occur as a response to precipitation events (Berthling & Etzelmüller, 2016), leading to the inwash of materials from the catchment. Furthermore, because of the low precipitation rates in the Arctic tundra, there is a relatively long residence time in Lake Sarsvatnet. This further allows these trace elements to accumulate in the lake.

There were also differences in trace element distribution within the lake. One factor influencing this could be the temperature gradient. Because of Svalbard's low temperatures, most Svalbard lakes are cold-monomictic (Brittain et al., 2020). Despite this, a gradual temperature gradient was observed on the sampling day from Lake Sarsvatnet's temperature data (Figure 8). Sufficient oxygen and a relatively well-mixed lake should favor a somewhat even vertical water chemistry as seen in other ultra-oligotrophic lakes (Cremer & Wagner, 2003). Although there were no oxygen measurements performed in this study, low concentration of dissolved Fe in the bottom waters (Figure 9) is indicative of a welloxygenated water column since Fe is released from the sediments at low oxygen concentrations (Wetzel, 2001, p. 295). However, several elements showed a variable distribution in the water column. Some of the variation could be explained by sampling errors, i.e., the sharp increase in the particulate fraction of most selected trace elements at 19 m. This was likely due to the water sampler that initiated resuspension of the sediments as indicated by the slightly higher turbidity value in the bottom lake sample (L6)(Table 2).

From the results, there was an enrichment of both dissolved and particulate Pb, Cu, Zn and Cd in the top layer (0.5 m) in Lake Sarsvatnet compared to the rest of the water column (Figure 15, Figure 16, Figure 17, Figure 18). As inlet stream concentrations were substantially lower than the top layer, there was no clear connection between the enrichment and the inputs from the catchment at the time of sampling. Although this study does not include data from before and after this precipitation event occurred, a plausible explanation could be the week-long precipitation event prior to sampling (Figure 7) that increased the flux of trace elements to the lake. Because the precipitation event ended five days before, this could explain why inlet stream concentrations were low at the time of sampling. The enrichment of the top layer (0.5 m) was likely a result of the weak thermal stratification which inhibited this water to mix with the rest of the water column.

4.2 Atmospheric deposition of sea salts and trace elements

Sea salts are brought to land with marine aerosols. In general, there is a decrease in Cl^--concentrations with distance from the sea (Skjelkvåle et al., 2001). The studied surface waters are close to the fjord (0 – 1.5 km), and it is therefore reasonable to assume they are influenced by sea salt deposition. The further assumption that all Cl^- present is from marine origin can give an indication on how strongly they are influenced by sea salts. However, the Cl-concentrations in the surface waters at Ossian Sars ranged from 4.8 mg/l to 5.9 mg/l, which is relatively low compared to other Arctic surface waters that reach up to 17.4 mg/l Cl^- (Dragon & Marciniak, 2010; Szumińska et al., 2018). Nonetheless, data from this study is similar to data from the Kongsfjorden area, including the rivers Londonelva and Bayelva (Krawczyk et al., 2003; Krawczyk & Pettersson, 2007).

In addition to Cl^-, marine aerosols also bring other ions present in sea water. The contribution of sea salts on the ion concentrations can be estimated by using the Cl/ion ratio in sea water, with the assumption that these are transported in the same ratio (Krawczyk & Pettersson, 2007; Szumińska et al., 2018). A high percentage of the total ion concentrations in this study was attributed to non-sea-salt (nss) sources for SO_4^{2-}, Ca^{2+}, Mg^{2+} and K^+ (Appendix G). This suggests a geogenic source to dominate the content of most major ions except Na^+ and Cl^-. The strong influence of rock weathering is in accordance with findings in the river Londonelva in Kongsfjorden, where Krawczyk and Pettersson (2007) found the main factor affecting ion chemistry in August was crustal weathering and that marine inputs had a low contribution.

A possible explanation for the relatively low impact of sea salts despite the proximity to the sea could be the prevailing wind direction in the area (Ny-Ålesund). These are dominated by northerly or easternly directions (Dekhtyareva et al., 2018; Pilguj et al., 2019) and therefore, most marine aerosols could be transported away from Ossian Sars. The Cl^- concentrations from this study is similar to other studies in Kongsfjorden. Differences within Svalbard could therefore be linked to regional differences in precipitation rates and the consequently different scavenging rates.

Atmospheric deposition to surface waters also includes naturally and anthropogenically derived contaminants (Kozak et al., 2015; Lehmann-Konera et al., 2021). Two of the tracers for atmospheric deposition, Cl^- and Br's, correlated strongly with PC2 (Figure 20). This suggests that this principal component explains the atmospheric signal in the PCA. Interestingly, Cd showed a weak positive correlation with PC2, which indicates that Cd in stream samples could be linked to atmospheric deposition.

Cd from atmospheric deposition has also been found by Zaborska et al. (2020) in the Hornsund fjord on Svalbard. The authors revealed high concentrations of Cd in August, likely as a result of higher atmospheric deposition load because of high precipitation rates. Regarding this study, the findings from Zaborska et al. (2020) may suggest that the precipitation events prior to sampling could be important in supplying toxic compounds into these surface waters. Although long-term air monitoring at the Zeppelin station in Ny-Ålesund have found a significant decrease in Cd concentrations from 1990 to 2020 (Bohlin-Nizzetto et al., 2021), there has been a small increase in Cd since 2007 (Platt et al., 2022). A proposed explanation for this is the erosion of newly ice-free areas and the subsequent transportation of wind-blown mineral dust. Therefore, the Cd from atmospheric deposition does not necessarily come from anthropogenic LRATP, but from a local source.

Ottesen et al. (2010, p. 44-45) conducted a geochemical mapping of Svalbard using overbank sediments. The authors revealed that the Br content in overbank sediments (the sediment deposited on the floodplain of a stream), at Ossian Sars are relatively high compared to other locations on Svalbard. This suggests that Br could also originate from a geological source and consequently weakening Br's suitability as a tracer for atmospheric deposition. However, overbank sediments are derived from the deposition of suspended stream particles. Thus, the possibility that the overbank sediment itself is influenced by atmospheric deposition is not to be neglected, as emphasized by Bølviken et al. (2004).

4.3 Geochemical factors influencing trace elements and pH

The Arctic is susceptible to chemical and physical rock weathering which represent a significant input of trace elements to surface waters. Most of the trace element concentrations in the streams fell in the range of other studies in surface waters on Svalbard, e.g. Szumińska et al. (2018) and Kozak et al. (2015). For lake samples, comparable data is only represented by grab samples. Therefore, comparisons were made with the top layer (L1). Although the existing literature is scarce, Kozak et al. (2016) and Ruman et al. (2021) reports substantially lower concentrations of Cu and Zn than found in Lake Sarsvatnet's top layer (Figure 15 & Figure 16).

Through a geochemical study of Svalbard lake sediments, Boyle et al. (2004) found elevated Cu and Zn concentrations in Lake Sarsvatnet's sediments compared to the other lakes in the study. In addition, high concentrations of Cu and Zn have also been reported from streams south-east in Kongsfjorden, where Hald (2014) suggested this to be caused by snowmelt and further drainage of the water through the mineral soil in the area. Taken together, this could indicate a common geological source for Zn and Cu in the inner part of Kongsfjorden in line with the conclusions from Boyle et al. (2004). For instance, both of these metals can be present in mica minerals (Ottesen et al., 2010, p. 69 & 146), which are important components of the local bedrock at Ossian Sars. However, this should be further investigated by detailed geochemical studies.

From the PCA, most trace elements correlated negatively with PC2 (Figure 20). As previously discussed, PC2 could represent the atmospheric signal in the data set. Because most trace elements correlated negatively with PC2, this implies that these originated from the catchment. This is further backed up by Ni and Co's strong positive correlation with most major ions (Appendix I) which originated from geological sources within the catchment based on their high nss-fraction. Ni and Co's negative correlation with other trace elements in the PCA could be explained by their different geological source or different transport mechanism in the streams.

In addition to being a source for trace elements, the geological substratum is responsible for the relatively high pH-values (~pH 8.0) in these surface waters. Similar pH-values (~pH 8.2) are found in other surface waters in Kongsfjorden with catchments dominated by the same carbonate bedrock (Krawczyk & Pettersson, 2007). Although the carbonate bedrock has a low coverage in the studied catchments (Figure 4), the high solubility of carbonates likely increases its impact on the water chemistry. For instance, Dragon and Marciniak (2010) pointed out the dissolution of calcareous rock as an important factor influencing the chemistry of Svalbard surface waters. This is because they are subject to extensive rock weathering in the harsh climate (Semkin et al., 2005).

pH is a key factor influencing trace element chemistry in surface waters. Because the solubility of metals is higher in acidic environments, the relatively high pH of these surface waters likely leads to low mobilization rates from the bedrock (Ryan, 2020, p. 117). In addition, the high pH increases the particle affinity of certain metals (Ryan, 2020, p. 248) which favors precipitation. Taken together, these factors could explain the low trace element concentrations in the streams. A small amount is mobilized from the bedrock and the fraction that is mobilized precipitates.

The metal's particle affinity could also help explain the accumulation of particulate Cu, Zn, Pb, Cd, Mn, and Fe in Lake Sarsvatnet compared to the streams (Figure 9, Figure 10, Figure 15, Figure 16, Figure 17, Figure 18). If so, the accumulated metals should have had a higher particle affinity compared to Ni, Co, Al and As that showed a more even distribution across the streams and lake (Figure 11, Figure 12, Figure 13, Figure 14). However, from literature (Ryan, 2020, p. 248), the metals Ni, Al and Co have similar particle affinities to the accumulated metals. Therefore, the previously discussed explanation where the accumulation could be a result of the inwash of a minerogenic material from the catchment is more plausible. Nonetheless, knowledge on the behavior and migration of these metals in this system requires a speciation study and is a task for further investigation.

4.4 Subsurface flow influencing major ion composition

Major ions typically related to the soil solution (Ca^{2+}, SO_4^{2-}, Mg^{2+}, Na^+ and K^+) had a strong positive correlation with PC1 (Figure 20), which suggest this principal component explains the influence of subsurface flow. From this, the north stream is the more affected than the inlet streams, indicating a higher contact time between the water in the north stream and its catchment. As ground temperatures near Ny-Ålesund reaches their maximum in mid-August (Christiansen et al., 2020, p. 243), the importance of subsurface flow likely increases throughout the summer. This is consistent with findings by Stutter and Billett (2003). The authors observed an increase in the input of soil solutes into stream waters throughout the summer because of biogeochemical processes enriching soil waters in the developing active layer.

When comparing results from this study with data from Birks et al. (2004b), there has been an increase in certain major ions in Lake Sarsvatnet since August 1995. Most strikingly, there has been a substantial increase in SO_4^{2-} concentrations (from 2.4 mg/l to 12.8 mg/l (sample O2)). Because long-term air monitoring in Ny-Ålesund has shown a significant decrease in the nss-sulfur content and are now considered low (Aas et al., 2021), the increase is not likely to be linked to present atmospheric deposition of SO_2.

A similar phenomenon is reported at several sites in the Arctic. A recent study from the Canadian High Arctic found a significant increase in lake SO_4^{2-} concentrations from 2006 to 2016 due to permafrost thaw (Roberts et al., 2017). Furthermore, findings from Keller et al. (2007) demonstrates that when the active layer deepens, minerals previously protected in the permafrost is susceptible to weathering. Although there are no data on long-term active layer development at Ossian Sars, it has generally deepened in the High Arctic (AMAP, 2017). Moreover, Keller et al. (2010) suggested that even a slight increase in the active layer could drastically alter the chemical composition of a Svalbard stream.

Because both the fieldwork for this study and Birks et al. (2004b) were executed in August, it suggests a long-term process influencing SO_4^{2-} concentrations. Based on the mentioned findings from Roberts et al. (2017) and Keller et al. (2010), this process could be the oxidation of previously protected pyrite minerals in the bedrock caused by a deepening of the active layer. Furthermore, the oxidation of sulfur is an acidifying process (Zak et al., 2021). If oxidation of reduced sulfuric compounds in the catchment explains the observed increase in SO_4^{2-}, it would be expected to lower the pH of the surface waters. However, due to the carbonate rich geological substratum, the alkalinity (Figure 19) could be high enough to buffer this process, and further maintaining the high pH. Taken together, this could explain the observed increase in SO_4^{2-} concentrations.

It should be emphasized that this observation is based on two snapshots of the water chemistry. Thus, if this observation is a result of anomalies in meteorological conditions or a significant temporal change cannot be established in this study. For instance, July of 2021 was substantially drier than normal, a condition that could have enhanced the drying of the catchment as the active layer deepened, and further improved the drainage and oxidized minerals. A multi-seasonal approach is therefore necessary for further research.

4.5 Lake Sarsvatnet's characteristics

As discussed, several factors influence the chemical features of Lake Sarsvatnet (Figure 21). The importance of the discussed factors could differ between lakes and consequently lead to large hydrochemical variations. Svalbard's high environmental variability makes it interesting to compare Lake Sarsvatnet's characteristics to other lakes on Svalbard. Based on the snapshot presented in this study, Lake Sarsvatnet holds similar characteristics to other Svalbard lakes. However, the concentrations of Cu and Zn (total of 60.74 µg/l and 43.08 µg/l respectively) were higher than reported by other lake studies.

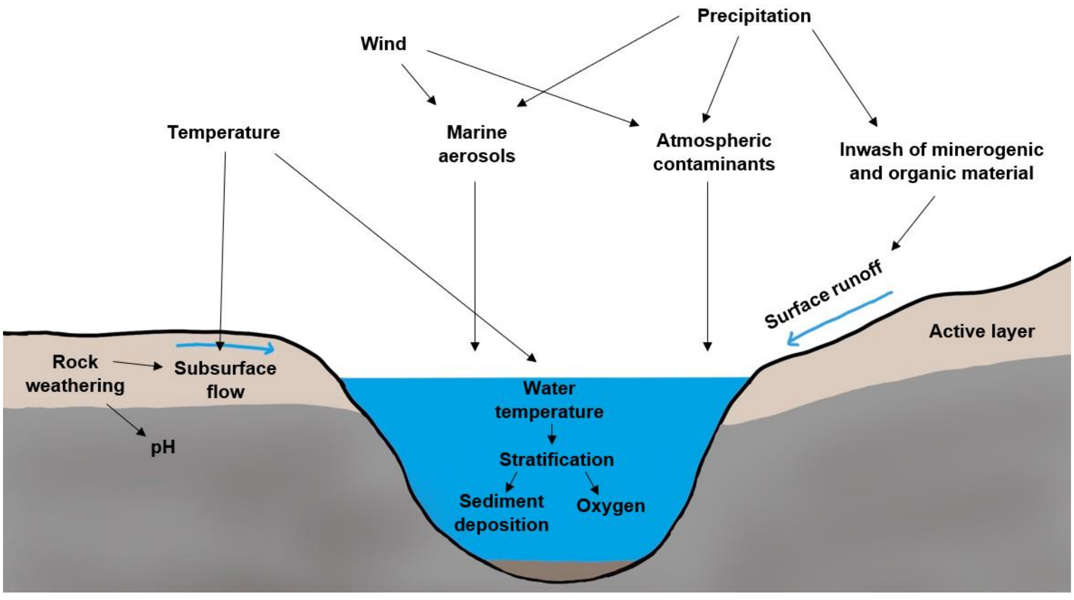

Figure 21: Graphical overview of key factors influencing Lake Sarsvatnet in August 2021 presented in this study.

The scarce vegetation leaves the lake low in organic matter (~2.0 mg/l TOC) as seen in e.g. Ruman et al. (2021) who found TOC-concentrations of <2.0 mg/l in Revvatnet. Based on the temperature data, Lake Sarsvatnet could not be considered a cold-monomictic lake as many other Svalbard lakes (Brittain et al., 2020). Furthermore, Svenning (2015) found temperatures reaching 14°C in some clearwater lakes in non-glaciated catchments because of compared to the 8°C in Lake Sarsvatnet.

Svalbard's geology varies greatly (Hjelle, 1993). As previously discussed, the influence of sea salts was diluted because of the high ion input from the geological substratum. Furthermore, the geological substratum leaves a neutral to alkaline pH in Lake Sarsvatnet which is assumed to be common on Svalbard (Brittain et al., 2020). The conductivity values found in Lake Sarsvatnet (186-198 µS/cm) fall in the middle range of other studies. Tundra lakes located on easily soluble gypsum and anhydrite can have values >550 µS/cm (Mazurek et al., 2012), while lakes on crystalline bedrock can reach values <10 µS/cm (Kozak et al., 2015).

4.6 Study limitations and future work

Freshwater chemistry is highly dynamic and data from this study only represents a snapshot of the studied surface waters. This makes it challenging to highlight the complex processes occurring, and the possibility of random errors is higher with this method compared to long-term studies. In addition, the inlet stream data are scarce. More sampling locations in the inlet streams would have given a deeper insight in sources than the current method using a stream in an adjacent catchment. Nonetheless, this snapshot study can help establish baseline conditions for further studies on how High Arctic catchments.

Although this study only aimed to map water chemistry in August, it is worth addressing that the timing of the sampling could have influenced the results. Findings from Rember and Trefry (2004) highlights the seasonal variations in trace element concentrations in surface waters. The authors reported higher stream concentrations of trace elements during spring due to melting of snow that has accumulated metals.

Because the external inputs of trace elements, e.g., from deposition of LRATP, are diluted by a strong geochemical signal, it is challenging to distinguish between sources. Besides, because of the dynamic characteristic of freshwater chemistry, Väisänen et al. (1998) suggested stream water not be an ideal substratum to map contamination. Precipitation samples would have increased the knowledge on the source of Cd, be it of geogenic or atmospheric origin.

Consequently, pollution studies including precipitation samples are recommended for future research. Lastly, with the projected increase in precipitation and the subsequent increase in erosion rates, increased sediment transport might be expected in the future (Hanssen-Bauer et al., 2019). The effect of seasonal variability and precipitation events on trace element and major ion concentration should be investigated.

5 Conclusions

The results presented in this study highlights the complexity of the interconnected factors influencing the chemical features of a non-glaciated High Arctic lake system. Factors influencing Lake Sarsvatnet's trace element and major ion composition in August of 2021 were found to be meteorological factors, rock weathering, atmospheric deposition, and the input of subsurface water flow. Lake Sarsvatnet showed similar characteristics of other Svalbard lakes, but higher concentrations of Zn and Cu. The PCA indicated that trace elements were mainly of geogenic origin, however, Cd could come from atmospheric deposition. In addition, the input of a minerogenic material from the catchment could be important in shaping the lake's trace element composition. Although Lake Sarsvatnet is located close to the fjord, the main source of most major ions is rock weathering. Because sampling was conducted in August, this source is likely enhanced by the active layer development throughout the summer.

This is the first study on the trace element composition of the Lake Sarsvatnet system and the study further contributes to the scarce data on the water chemistry of Svalbard's surface waters. The study revealed the potential influence of permafrost thaw and deposition of toxic metals on Arctic catchments. However, this study did not aim at exploring inter-seasonal or multi-seasonal variations in water chemistry. Following Arctic's fast changing climate, there is still a high need for a deeper understanding on freshwater systems response to human-induced changes. Future research is therefore needed to understand the long-term effects of these changes on the fragile Arctic freshwater systems.

References

AMAP. (1998). *AMAP Assessment Report: Arctic Pollution Issues*. Oslo, Norway: Arctic Monitoring and Assessment Programme (AMAP). Available at: https://www.amap.no/documents/doc/amap-assessment-report-arctic-pollution-issues/68 (accessed: 26.03.2022).

AMAP. (2016). *Influence of Climate Change on Transport, Levels, and Effects of Contaminants in Northern Areas – Part 2*. Oslo, Norway: Arctic Monitoring and Assessment Programme (AMAP). Available at: https://www.amap.no/documents/doc/influence-of-climate-change-on-transport-levels-and-effects-of-contaminants-in-northern-areas-part-2/1561 (accessed: 21.04.2021).

AMAP. (2017). *Snow, Water, Ice and Permafrost in the Arctic (SWIPA) 2017*. Oslo, Norway: Arctic Monitoring and Assessment Programme (AMAP). Available at: https://www.amap.no/documents/doc/snow-water-ice-and-permafrost-in-the-arctic-swipa-2017/1610 (accessed: 16.04.2021).

Appleby, P. G. (2004). Environmental Change and Atmospheric Contamination on Svalbard: Sediment Chronology. *Journal of Paleolimnology*, 31 (4): 433-443. doi: 10.1023/B:JOPL.0000022545.73163.ed.

Berthling, I. & Etzelmüller, B. (2016). The changing cryosphere - implications for solute and sedimentary fluxes in cold climate environments. In Achim, A. B., John, C. D. & Zbigniew, Z. (eds) *Source-to-Sink Fluxes in Undisturbed Cold Environments*. Cambridge: Cambridge University Press.

Bindler, R., Renberg, I., John Anderson, N., Appleby, P. G., Emteryd, O. & Boyle, J. (2001). Pb isotope ratios of lake sediments in West Greenland: inferences on pollution sources. *Atmospheric environment (1994)*, 35 (27): 4675-4685. doi: 10.1016/S1352-2310(01)00115-7.

Birks, H. J. B., Jones, V. J. & Rose, N. L. (2004a). Recent Environmental Change and Atmospheric Contamination on Svalbard as Recorded in Lake Sediments – Synthesis and General Conclusions. *Journal of Paleolimnology*, 31 (4): 531-546. doi: 10.1023/B:JOPL.0000022550.81129.1a.

Birks, H. J. B., Monteith, D. T., Rose, N. L., Jones, V. J. & Peglar, S. M. (2004b). Recent Environmental Change and Atmospheric Contamination on Svalbard as Recorded in Lake Sediments – Modern Limnology, Vegetation, and Pollen Deposition. *Journal of Paleolimnology*, 31 (4): 411-431. doi: 10.1023/B:JOPL.0000022543.03382.fa.

Bjerkås, A. B. (2019). *Holocen rekonstruksjon av Kongsbreen, Svalbard*. Master's Thesis Bergen: University of Bergen. Available at: https://hdl.handle.net/1956/20444 (accessed: 03.03.2022).

Blaen, P. J., Hannah, D. M., Brown, L. E. & Milner, A. M. (2014). Water source dynamics of high Arctic river basins. *Hydrological Processes*, 28 (10): 3521-3538. doi: 10.1002/hyp.9891.

Bohlin-Nizzetto, P., Aas, W., Halvorsen, H. L., Nikiforov, V. & Pfaffhuber, K. A. (2021). *Monitoring of environmental contaminants in air and precipitation. Annual report 2020*. NILU report 12/2021: Norwegian Institute for Air Research (NILU). Available at: https://nilu.brage.unit.no/nilu-xmlui/handle/11250/2778509 (accessed: 15.02.2022).

Boyle, J. F., Rose, N. L., Appleby, P. G. & Birks, H. J. B. (2004). Recent Environmental Change and Human Impact on Svalbard: The Lake-Sediment Geochemical Record. *Journal of Paleolimnology*, 31 (4): 515-530. doi: 10.1023/B:JOPL.0000022549.07298.6e.

Brittain, J. E., Schartau, A. K. & Svenning, M.-A. (2020). *Biologisk mangfold i ferskvann på Svalbard: kunnskapsgrunnlag, påvirkninger og forslag til framtidig overvåking*. Rapport nr. 13/2020: Norges vassdrags- og energidirektorat Available at: http://publikasjoner.nve.no/rapport/2020/rapport2020_13.pdf (accessed: 17.04.2021).

Bølviken, B., Bogen, J., Jartun, M., Langedal, M., Ottesen, R. T. & Volden, T. (2004). Overbank sediments: A natural bed blending sampling medium for large-scale geochemical mapping. *Chemometrics and Intelligent Laboratory Systems*, 74: 183-199. doi: 10.1016/j.chemolab.2004.06.006.

Christiansen, H., Gilbert, G., Demidov, N., Guglielmin, M., Isaksen, K., Osuch, M. & Boike, J. (2020). Permafrost temperatures and active layer thickness in Svalbard during 2017/2018 (PermaSval). In *SESS Report 2019 - The State of Environmental Science in Svalbard*, pp. 236-249: Svalbard Integrated Arctic Earth Observing System (SIOS).

CliC/AMAP/IASC. (2016). *The Arctic Freshwater System in a Changing Climate*: WCRP Climate and Cryosphere (CliC) Project, Arctic Monitoring and Assessment Programme (AMAP), International Arctic Science Committee (IASC). Available at: https://www.amap.no/documents/doc/the-arctic-freshwater-system-in-a-changing-climate/1375 (accessed: 05.10.2021).

Côté, G., Pienitz, R., Velle, G. & Wang, X. (2010). Impact of Geese on the Limnology of Lakes and Ponds from Bylot Island (Nunavut, Canada). *International Review of Hydrobiology*, 95 (2): 105-129. doi: 10.1002/iroh.200911151.

Cremer, H. & Wagner, B. (2003). The diatom flora in the ultra-oligotrophic Lake El'gygytgyn, Chukotka. *Polar Biology*, 26 (2): 105-114. doi: 10.1007/s00300-002-0445-0.

Dallmann, W. K. (2015). *Geoscience Atlas of Svalbard*. Report series No. 148: Norwegian Polar Institute Available at: http://hdl.handle.net/11250/2580810 (accessed: 14.01.2022).
Dekhtyareva, A., Holmén, K., Maturilli, M., Hermansen, O. & Graversen, R. (2018). Effect of seasonal mesoscale and microscale meteorological conditions in Ny-Ålesund on results of monitoring of long-range transported pollution. *Polar research*, 37 (1): 1508196. doi: 10.1080/17518369.2018.1508196.
Digernes, I. (2004). *Kjemiske og fysikalske metoder for måling i vann*. Ås: Norwegian University of Life Sciences
Dommergue, A., Larose, C., Faïn, X., Clarisse, O., Foucher, D., Hintelmann, H., Schneider, D. & Ferrari, C. P. (2010). Deposition of Mercury Species in the Ny-Ålesund Area (79°N) and Their Transfer during Snowmelt. *Environmental Science & Technology*, 44 (3): 901-907. doi: 10.1021/es902579m.
Dragon, K. & Marciniak, M. (2010). Chemical composition of groundwater and surface water in the Arctic environment (Petuniabukta region, central Spitsbergen). *Journal of Hydrology*, 386 (1): 160-172. doi: 10.1016/j.jhydrol.2010.03.017.
Forskrift om Ossian Sars naturreservat. (2003). *Forskrift om fredning av Ossian Sars naturreservat av 26. september 2003 nr. 1188*. Available at: https://lovdata.no/dokument/SF/forskrift/2003-09-26-1188 (accessed: 16.04.2022).
Hald, S. J. K. (2014). *Kartlegging og studie av metaller og naturlig organisk materiale i elver på Svalbard*. Master's Thesis. Trondheim: Norwegian University of Science and Technology. Available at: http://hdl.handle.net/11250/2351949 (accessed: 19.04.2022).
Hall, K., Thorn, C. E., Matsuoka, N. & Prick, A. (2002). Weathering in cold regions: some thoughts and perspectives. *Progress in Physical Geography: Earth and Environment*, 26 (4): 577-603. doi: 10.1191/0309133302pp353ra.
Hamilton, P. B., Gajewski, K., Atkinson, D. E. & Lean, D. R. S. (2001). Physical and chemical limnology of 204 lakes from the Canadian Arctic Archipelago. *Hydrobiologia*, 457 (1): 133-148. doi: 10.1023/A:1012275316543.
Hanssen-Bauer, I., Førland, E. J., Hisdal, H., Mayer, S., Sandø, A. B. & Sorteberg, A. (2019). *Climate in Svalbard 2100 - a knowledge base for climate adaption* NCCS report 1/2019: Norwegian Environment Agency. Available at: https://www.miljodirektoratet.no/publikasjoner/2019/februar-2019/climate-in-svalbard-2100--a-knowledge-base-for-climate-adaptation/ (accessed: 13.03.2022).
Hjelle, A. (1993). *Geology of Svalbard*. Polarhåndbok no. 7: Norwegian Polar Institute. Available at: http://hdl.handle.net/11250/216668 (accessed: 14.01.2022).
Hjelle, A., Piepjohn, K., Saalmann, K., Ohta, Y., Salvigsen, O., Thiedig, F. & Dallmann, W. K. (1999). Geological Map of Svalbard 1:100,000. Sheet A7G Kongsfjorden. *Norsk Polarinstitutt Temakart*, Nr. 30: 56 p.
Huser, B. J., Futter, M. N., Bogan, D., Brittain, J. E., Culp, J. M., Goedkoop, W., Gribovskaya, I., Karlsson, J., Lau, D. C. P., Rühland, K. M., et al. (2022). Spatial and temporal variation in Arctic freshwater chemistry—Reflecting climate-induced landscape alterations and a changing template for biodiversity. *Freshwater Biology*, 67 (1): 14-29. doi: 10.1111/fwb.13645.
Kalff, J. (2002). *Limnology: inland water ecosystems* Upper Saddle River, N.J.: Patience Hall.
Keller, K., Blum, J. D. & Kling, G. W. (2007). Geochemistry of Soils and Streams on Surfaces of Varying Ages in Arctic Alaska. *Arctic, Antarctic, and Alpine Research*, 39 (1): 84-98. doi: 10.1657/1523-0430(2007)39[84:GOSASO]2.0.CO;2.
Keller, K., Blum, J. D. & Kling, G. W. (2010). Stream geochemistry as an indicator of increasing permafrost thaw depth in an arctic watershed. *Chem. Geol.*, 273: 76-81. doi: 10.1016/j.chemgeo.2010.02.013.
Kozak, K., Kozioł, K., Luks, B., Chmiel, S., Ruman, M., Marć, M., Namieśnik, J. & Polkowska, Ż. (2015). The role of atmospheric precipitation in introducing contaminants to the surface waters of the Fuglebekken catchment, Spitsbergen. *Polar research*, 34 (1): 24207-10. doi: 10.3402/polar.v34.24207.
Kozak, K., Polkowska, Ż., Stachnik, Ł., Luks, B., Chmiel, S., Ruman, M., Lech, D., Kozioł, K., Tsakovski, S. & Simeonov, V. (2016). Arctic catchment as a sensitive indicator of the environmental changes: distribution and migration of metals (Svalbard). *International Journal of Environmental Science and Technology*, 13 (12): 2779-2796. doi: 10.1007/s13762-016-1137-6.
Krawczyk, W. E., Lefauconnier, B. & Pettersson, L.-E. (2003). Chemical denudation rates in the Bayelva Catchment, Svalbard, in the Fall of 2000. *Physics and Chemistry of the Earth, Parts A/B/C*, 28 (28): 1257-1271. doi: https://doi.org/10.1016/j.pce.2003.08.054.
Krawczyk, W. E. & Pettersson, L.-E. (2007). Chemical denudation rates and carbon dioxide drawdown in an ice-free polar karst catchment: Londonelva, Svalbard. *Permafrost Periglac. Process*, 18 (4): 337-350. doi: 10.1002/ppp.599.
Law, K. S. & Stohl, A. (2007). Arctic Air Pollution: Origins and Impacts. *Science*, 315 (5818): 1537-1540. doi: 10.1126/science.1137695.

Laybourn-Parry, J. & Marshall, W. A. (2003). Photosynthesis, mixotrophy and microbial plankton dynamics in two high Arctic lakes during summer. *Polar Biology*, 26 (8): 517-524. doi: 10.1007/s00300-003-0514-z.

Lehmann-Konera, S., Kociuba, W., Chmiel, S., Franczak, L. & Polkowska, Z. (2021). Effects of biotransport and hydro-meteorological conditions on transport of trace elements in the Scott River (Bellsund, Spitsbergen). *PeerJ*, 9: e11477. doi: 10.7717/peerj.11477.

Lewis, T., Lafrenière, M. J. & Lamoureux, S. F. (2012). Hydrochemical and sedimentary responses of paired High Arctic watersheds to unusual climate and permafrost disturbance, Cape Bounty, Melville Island, Canada. *Hydrological Processes*, 26 (13): 2003-2018. doi: 10.1002/hyp.8335.

Lindström, E. & Leskinen, E. (2002). Do neighboring lakes share common taxa of bacterioplankton? Comparison of 16S rDNA fingerprints and sequences from three geographic regions. *Microbial ecology*, 44: 1-9. doi: 10.1007/s00248-002-0007-6.

Macdonald, R. W., Barrie, L. A., Bidleman, T. F., Diamond, M. L., Gregor, D. J., Semkin, R. G., Strachan, W. M. J., Li, Y. F., Wania, F., Alaee, M., et al. (2000). Contaminants in the Canadian Arctic: 5 years of progress in understanding sources, occurrence and pathways. *Science of The Total Environment*, 254 (2): 93-234. doi: 10.1016/S0048-9697(00)00434-4.

Macdonald, R. W., Harner, T. & Fyfe, J. (2005). Recent climate change in the Arctic and its impact on contaminant pathways and interpretation of temporal trend data. *Science of The Total Environment*, 342 (1): 5-86. doi: 10.1016/j.scitotenv.2004.12.059.

Mazurek, M., Renata, P., Rachlewicz, G. & Zwolinski, Z. (2012). Variability of Water Chemistry in Tundra Lakes, Petuniabukta Coast, Central Spitsbergen, Svalbard. *TheScientificWorldJournal*, 2012: 596516. doi: 10.1100/2012/596516.

Moiseenko, T. & Gashkina, N. (2020). Distribution and bioaccumulation of heavy metals (Hg, Cd and Pb) in fish: Influence of the aquatic environment and climate. *Environmental Research Letters*, 15 (11): 115013. doi: 10.1088/1748-9326/abbf7c.

Molau, U. (2016). Changes in vegetation cover and implications for solute and sedimentaryfluxes in cold climate environments. In Achim, A. B., John, C. D. & Zbigniew, Z. (eds) *Source-to-Sink Fluxes in Undisturbed Cold Environments*, pp. 30-35. Cambridge: Cambridge University Press.

Norsk Klimaservicesenter. (n.d.). *Observasjoner og værstatistikk*: Norsk Klimaservicesenter. Available at: https://seklima.met.no/observations/ (accessed: 13.04.2022).

Norwegian Polar Institute. (2013). *NP Basiskart Svalbard WMTS 25833 [Data set]*. Available at: https://geodata.npolar.no/ (accessed: 10.03.2022).

Norwegian Polar Institute. (2014a). *Kartdata Svalbard 1:100 000 (S100 Kartdata) / Map Data [Data set]*. Available at: https://doi.org/10.21334/npolar.2014.645336c7 (accessed: 10.03.2022).

Norwegian Polar Institute. (2014b). *Terrengmodell Svalbard (S0 Terrengmodell) [Data set]*. Available at: https://doi.org/10.21334/npolar.2014.dce53a47 (accessed: 11.03.2022).

Norwegian Polar Institute. (2016a). *Geological map of Svalbard (1:250000) [Data set]*. Available at: https://doi.org/10.21334/npolar.2016.616f7504 (accessed: 11.03.2022).

Norwegian Polar Institute. (2016b). *NP Ortofoto Svalbard WMTS 25833 [Data set]*. Available at: https://geodata.npolar.no/.

Ottesen, R. T., Bogen, J. & Finne, T. E. (2010). *Geochemical atlas of Norway - Part 2: Geochemical atlas of Spitsbergen*. Trondheim: Geological Survey of Norway and Norges vassdrags- og energidirektorat.

Pilguj, N., Kolendowicz, L., Kryza, M., Migała, K. & Czernecki, B. (2019). Temporal changes in wind conditions at Svalbard for the years 1986–2015. *Geografiska Annaler: Series A, Physical Geography*, 101 (2): 136-156. doi: 10.1080/04353676.2019.1572973.

Platt, S. M., Hov, Ø., Berg, T., Breivik, K., Eckhardt, S., Eleftheriadis, K., Evangeliou, N., Fiebig, M., Fisher, R., Hansen, G., et al. (2022). Atmospheric composition in the European Arctic and 30 years of the Zeppelin Observatory, Ny-Ålesund. *Atmos. Chem. Phys.*, 22 (5): 3321-3369. doi: 10.5194/acp-22-3321-2022.

Polkowska, Ż., Cichała-Kamrowska, K., Ruman, M., Kozioł, K., Krawczyk, W. E. & Namieśnik, J. (2011). Organic Pollution in Surface Waters from the Fuglebekken Basin in Svalbard, Norwegian Arctic. *Sensors*, 11 (9): 8910-8929. doi: 10.3390/s110908910.

Rember, R. D. & Trefry, J. H. (2004). Increased concentrations of dissolved trace metals and organic carbon during snowmelt in rivers of the alaskan arctic. *Geochimica et cosmochimica acta*, 68 (3): 477-489. doi: 10.1016/S0016-7037(03)00458-7.

Roberts, K. E., Lamoureux, S. F., Kyser, T. K., Muir, D. C. G., Lafrenière, M. J., Iqaluk, D., Pieńkowski, A. J. & Normandeau, A. (2017). Climate and permafrost effects on the chemistry and ecosystems of High Arctic Lakes. *Scientific Reports*, 7 (1): 13292. doi: 10.1038/s41598-017-13658-9.

Rudnicka-Kępa, P. & Zaborska, A. (2021). Sources, fate and distribution of inorganic contaminants in the Svalbard area, representative of a typical Arctic critical environment–a review. *Environmental Monitoring and Assessment*, 193 (11): 724. doi: 10.1007/s10661-021-09305-6.

Ruman, M., Kosek, K., Koziol, K., Ciepły, M., Kozak-Dylewska, K. & Polkowska, Ż. (2021). A High-Arctic flow-through lake system hydrochemical changes: Revvatnet, southwestern Svalbard (years 2010–2018). *Chemosphere*, 275: 130046. doi: 10.1016/j.chemosphere.2021.130046.
Ryan, P. (2020). *Environmental and Low-Temperature Geochemistry*. 2nd ed. Hoboken, NJ: Wiley Blackwell
Semkin, R. G., Mierle, G. & Neureuther, R. J. (2005). Hydrochemistry and mercury cycling in a High Arctic watershed. *Science of The Total Environment*, 342 (1): 199-221. doi: 10.1016/j.scitotenv.2004.12.047.
Skjelkvåle, B. L., Henriksen, A., Jònsson, G. S., Mannio, J., Wilander, A., Jensen, J. P., Fjeld, E. & Lien, L. (2001). *Chemistry of lakes in the Nordic region - Denmark, Finland with Åland, Iceland, Norway with Svalbard and Bear Island, and Sweden*. Report SNO 4391-2001: Norwegian Institute for Water REsearch (NIVA). Available at: http://hdl.handle.net/11250/211308 (accessed: 06.02.2022).
Stutter, M. I. & Billett, M. F. (2003). Biogeochemical controls on streamwater and soil solution chemistry in a High Arctic environment. *Geoderma*, 113 (1): 127-146. doi: 10.1016/S0016-7061(02)00335-X.
Svenning, M.-A. (2015). *Miljøvariable i innsjøer på Svalbard*. NINA Minirapport 575. Available at: https://www.miljovernfondet.no/wp-content/uploads/2020/02/12-80-rapport-miljovariable-i-innsjoer-pa-svalbard.pdf (accessed: 05.05.2022).
Szumińska, D., Szopińska, M., Lehmann-Konera, S., Franczak, Ł., Kociuba, W., Chmiel, S., Kalinowski, P. & Polkowska, Ż. (2018). Water chemistry of tundra lakes in the periglacial zone of the Bellsund Fiord (Svalbard) in the summer of 2013. *Science of The Total Environment*, 624: 1669-1679. doi: 10.1016/j.scitotenv.2017.10.045.
Väisänen, U., Misund, A. & Chekushin, V. (1998). Ecogeochemical Investigation: Stream Water Quality as an Indicator of Pollution in the Border Areas of Finland, Norway and Russia. *Water, Air, and Soil Pollution*, 104 (1): 205-219. doi: 10.1023/A:1004901016805.
Wawrzyniak, T. & Osuch, M. (2020). A 40-year High Arctic climatological dataset of the Polish Polar Station Hornsund (SW Spitsbergen, Svalbard). *Earth System Science Data*, 12: 805-815. doi: 10.5194/essd-12-805-2020.
Wetzel, R. G. (2001). *Limnology*. 3rd ed. San Diego: Academic Press.
White, D., Hinzman, L., Alessa, L., Cassano, J., Chambers, M., Falkner, K., Francis, J., Gutowski Jr., W. J., Holland, M., Holmes, R. M., et al. (2007). The arctic freshwater system: Changes and impacts. *Journal of Geophysical Research: Biogeosciences*, 112 (G4). doi: 10.1029/2006JG000353.
Yang, Z., Zhang, Y., Xie, Z., Wang, J., Li, Z., Li, Y., Du, J. & Sun, L. (2021). Potential influence of rapid climate change on elemental geochemistry distributions in lacustrine sediments—A case study at a high Arctic site in Ny-Ålesund, Svalbard. *Science of The Total Environment*, 801: 149784. doi: 10.1016/j.scitotenv.2021.149784.
Zaborska, A., Strzelewicz, A., Rudnicka, P. & Moskalik, M. (2020). Processes driving heavy metal distribution in the seawater of an Arctic fjord (Hornsund, southern Spitsbergen). *Marine Pollution Bulletin*, 161: 111719. doi: 10.1016/j.marpolbul.2020.111719.
Zak, D., Hupfer, M., Cabezas, A., Jurasinski, G., Audet, J., Kleeberg, A., McInnes, R., Kristiansen, S. M., Petersen, R. J., Liu, H., et al. (2021). Sulphate in freshwater ecosystems: A review of sources, biogeochemical cycles, ecotoxicological effects and bioremediation. *Earth-Science Reviews*, 212: 103446. doi: 10.1016/j.earscirev.2020.103446.
Aas, W., Eckhardt, S., Fiebig, M., Platt, S. M., Solberg, S., Yttri, K. E. & Zwaaftink, C. G. (2021). *Monitoring of long-range transported air pollutants in Norway. Annual Report 2020*. NILU report 13/2021: NILU. Available at: https://nilu.brage.unit.no/nilu-xmlui/handle/11250/2767251 (accessed: 03.03.2022).

Appendix

Appendix A. – Estimated residence time

To calculate the water residence time for Lake Sarsvatnet, the equation listed below was used. Because evaporation and input of snow melt is not included in the equation, this number is uncertain and only represents a rough estimate on lake residence time.

$$Estimated\ residence\ time = \frac{Volume}{Input} = \frac{Mean\ depth\ \times Lake\ size}{Annual\ precipitation\ \times Catchment\ size}$$

Annual precipitation normal (1991-2020) = 468 mm/year

Mean depth = 11 m (Appleby, 2004)

Lake size = 0.22 km^2

Catchment size = 1.3 km^2

Appendix B. – Vegetation map

Vegetation map of Ossian Sars. English translations from *Svalbardkartet* (n.d.) and data set from Johansen et al. (2009).

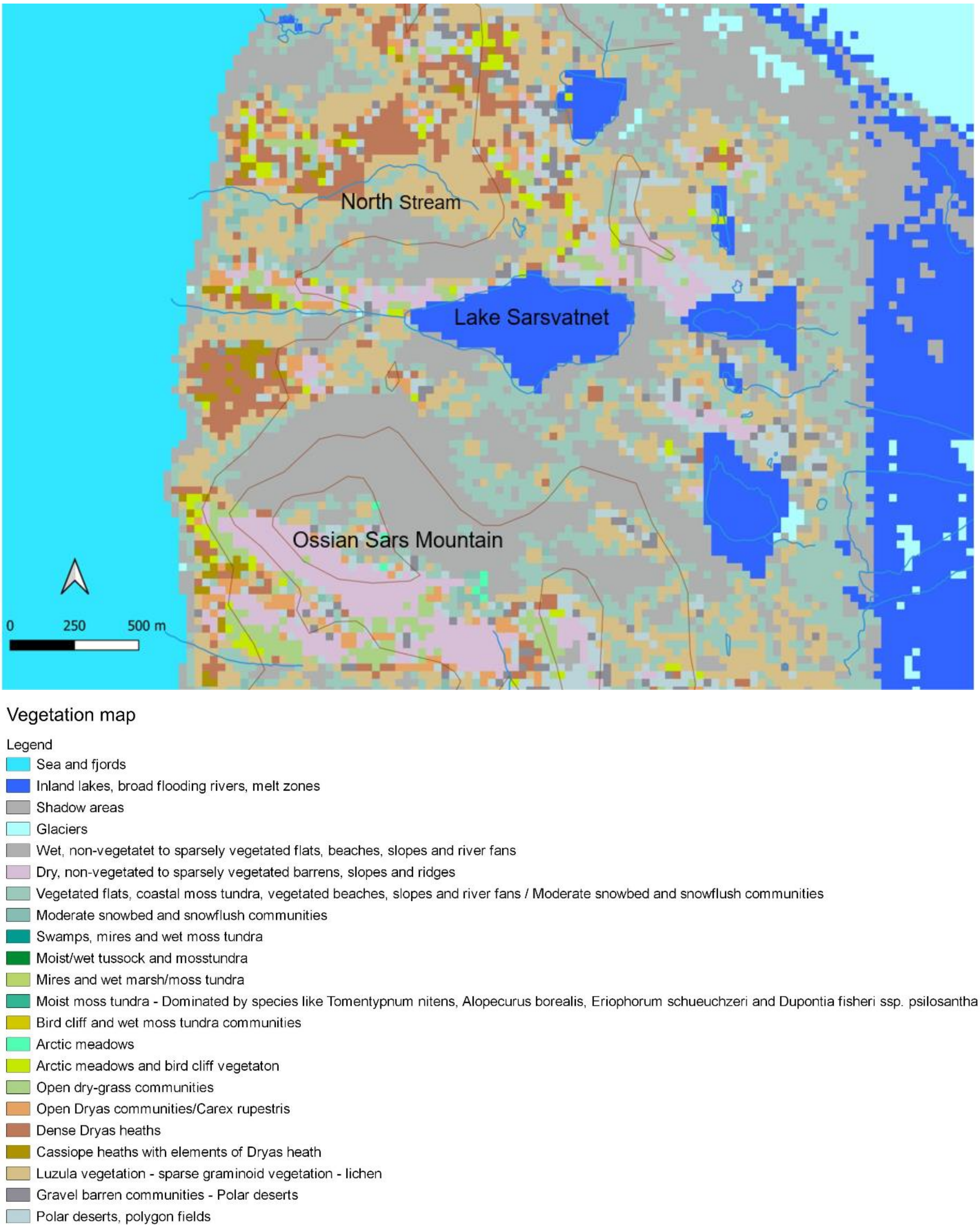

Appendix C. – Pictures from fieldwork

Pictures of one of the inlet streams (A), the north stream (B), the outlet stream (C) and lake Sarsvatnet taken from the west side of the lake (D). Photo: Lill Katrin Gorseth.

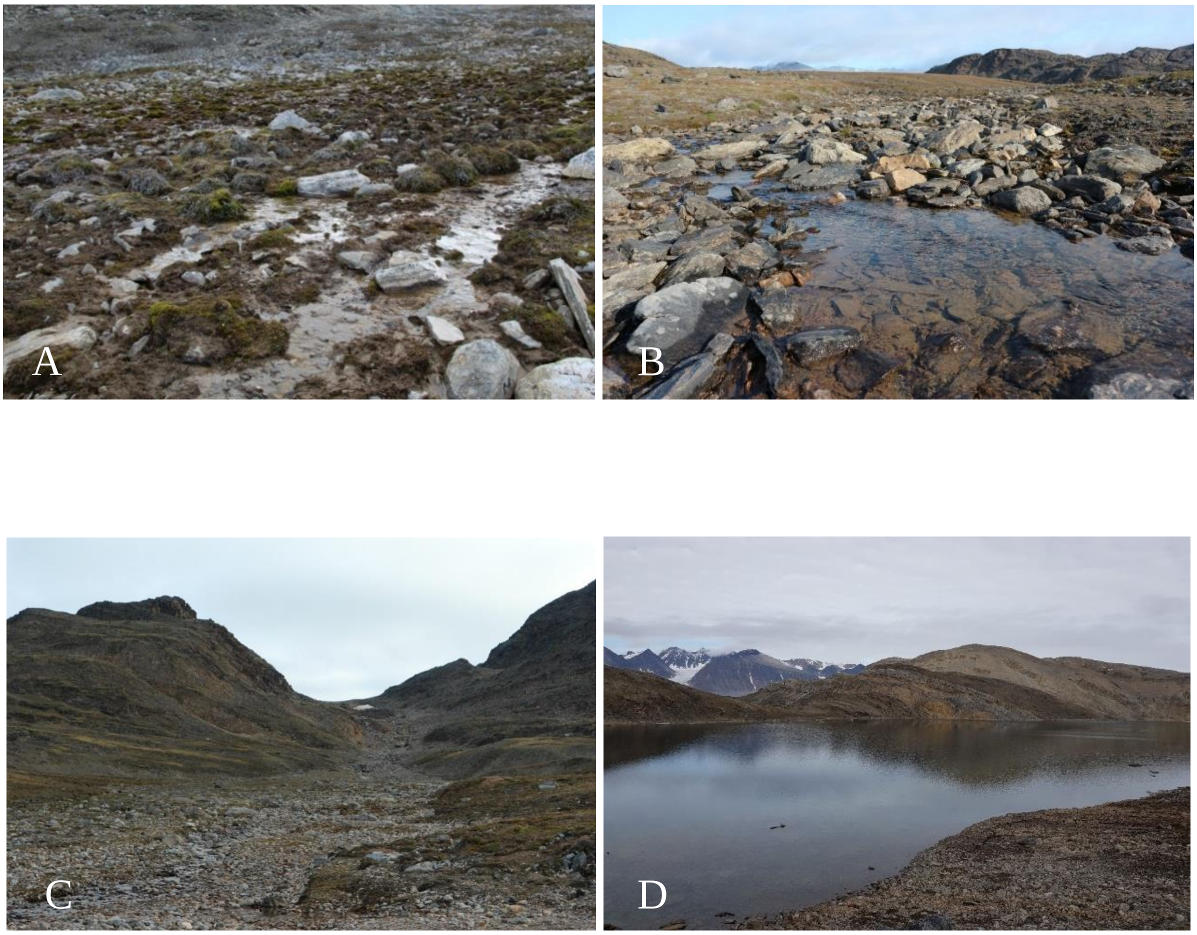

Appendix D. – Coordinates for sampling locations

Coordinates for sampling locations at Ossian Sars from fieldwork on August 18th and 19th 2021. Locations for sampling in Lake Sarsvatnet (L1-L6), its inlet streams (I1 and I2), outlet stream (O1-O8) and the north stream (N1-N4) are listed.

Sample	Coordinates
L1-L6	78.94970°N 12.49878°E
I1	78.94830°N 12.49627°E
I2	78.94928°N 12.49212°E
O1	78.95072°N 12.47528°E
O2	78.95090°N 12.46660°E
O3	78.95090°N 12.46565°E
O4	78.95082°N 12.46408°E
O5	78.95080°N 12.45655°E
O6	78.95070°N 12.44957°E
O7	78.95067°N 12.44010°E
O8	78.95082°N 12.43393°E
N1	78.95450°N 12.45687°E
N2	78.95483°N 12.44958°E
N3	78.95495°N 12.44317°E
N4	78.95468°N 12.43748°E

Appendix E. – Overbank sediment

E.1 Materials and methods

An overbank sediment sample (OBS) from the top few centimeters of an overbank sediment was collected from the outlet stream (78.95065°N 12.44012°E) in a 50 mL metal free plastic tube. This was analyzed with an Agilent 8800 Tripple Quadrupole ICP-MS. Before analyzation by ICP-MS, the overbank sediment was freeze dried for five days. This was to ensure a homogenized sample. Following this, the sample was added 50% HNO3 v/v before digestion in a Milestone UltraCLAVE an further dilution with Milli-Q water. Lastly, 15 mL of the digested and diluted sample was transferred to PP-tubes before ICP-MS analysis.

E.2 Raw data from ICP-MS

Primary data from ICP-MS analysis on the overbank sediment collected from Lake Sarsvatnet's outlet stream on August 19th.

Sample	Li	Be	B [H2]	B [O2]	Na	Mg	Al	Si	P	S	Cl	K	Ca	Sc	Ti	V	Cr
	[mg/g]	[μg/g]	[μg/g]	[μg/g]	[μmg/g]	[mg/g]	[mg/g]	[mg/g]	[mg/g]	[mg/g]	[mg/g]	[mg/g]	[mg/g]	[μg/g]	[mg/g]	[μg/g]	[μg/g]
OBS	23.60	1.67	10.76	9.67	0.31	10.79	27.38	2.15	0.39	0.30	<LOD	9.41	15.02	6.88	0.73	37.51	29.06

Sample	Mn	Fe	Co	Ni	Cu	Zn	Ga	As	Se	Br	Rb	Sr	Y	Zr	Nb	Mo
	[mg/g]	[mg/g]	[μg/g]	[μg/g]	[μg/g]	[μg/g]	[μg/g]	[μg/g]	[μg/g]	[μg/g]	[mg/g]	[μg/g]	[μg/g]	[μg/g]	[μg/g]	[μg/g]
OBS	0.56	25.41	10.30	18.27	17.90	52.37	10.09	3.63	1.00	14.77	0.06	22.93	14.59	5.59	0.02	0.15

Sample	Ru	Pd	Cd	In	Sn	Sb	Cs	Ba	La	Ce	Pr	Nd	Sm	Eu	Gd	Tb
	[μg/g]	[μg/g]	[μg/g]	[μg/g]	[μg/g]	[μg/g]	[μg/g]	[mg/g]	[μg/g]	[μg/g]	[μg/g]	[μg/g]	[μg/g]	[μg/g]	[μg/g]	[μg/g]
OBS	<LOD	0.16	0.06	0.03	0.19	0.01	4.17	0.14	35.69	78.63	9.29	36.31	6.79	0.83	5.55	0.70

Sample	Dy	Ho	Er	Tm	Yb	Lu	Hf	Ta	W	Pt	Hg	Tl	Pb	Bi	Th	U
	[μg/g]	[μg/g]	[μg/g]	[μg/g]	[μg/g]	[μg/g]	[μg/g]	[μg/g]	[μg/g]	[μg/g]	[μg/g]	[μg/g]	[μg/g]	[μg/g]	[μg/g]	[μg/g]
OBS	3.44	0.58	1.43	0.18	1.14	0.15	0.18	<LOD	<LOD	<LOD	<LOD	0.36	8.25	0.17	9.45	1.72

E.3 Detection limits ICP-MS

Detection limits (LOD) for the overbank sediment listed in µg/l for elements analyzed by ICP-MS.

Name	LOD (µg/l)	Name	LOD (µg/l)	Name	LOD (µg/l)
Li	0.0043	Br	0.2928	Cs	0.0005
Be	0.0000	Rb	0.0006	Ba	0.0024
B [H2]	0.1786	Sr	0.0015	La	0.0000
B [O]	0.0045	Y	0.0001	Ce	0.0000
Na	0.1050	Zr	0.0004	Pr	0.0000
Mg	0.0040	Nb	0.0001	Nd	0.0001
Al	0.0041	Mo	0.0013	Sm	0.0001
Si	0.1390	Ru	0.0017	Eu	0.0000
P	0.0132	Pd	0.0007	Gd	0.0001
S	0.1380	Cd	0.0003	Tb	0.0000
Cl	95.6709	In	0.0001	Dy	0.0001
K	0.0619	Sn	0.0005	Ho	0.0000
Ca	0.0215	Sb	0.0005	Er	0.0000
Sc	0.0025	Cs	0.0005	Tm	0.0000
Ti	0.0028	Ba	0.0024	Yb	0.0001
V	0.0010	La	0.0000	Lu	0.0000
Cr	0.0018	Ce	0.0000	Hf	0.0001
Mn	0.0015	Pr	0.0000	Ta	0.0000
Fe	0.0062	Nd	0.0001	W	0.0007
Co	0.0011	Mo	0.0013	Pt	0.0010
Ni	0.0007	Ru	0.0017	Hg	0.0079
Cu	0.0036	Pd	0.0007	Tl	0.0003
Zn	0.0103	Cd	0.0003	Pb	0.0002
Ga	0.0004	In	0.0001	Bi	0.0005
As	0.0005	Sn	0.0005	Th	0.0008
Se	0.0074	Sb	0.0005	U	0.0002

Appendix F. – Raw data from ICP-MS

F.1 Filtered water samples

Raw data from laboratory analyses on filtered (0.45 µm) water samples collected at Ossian Sars on August 18th (I1, I2, L1-L6 and O1-O6) and August 19th, 2021 (O7, O8 and N1-N4).

Sample	Li (µg/l)	Be (µg/l)	B (µg/l)	Na (µg/l)	Mg (µg/l)	Al (µg/l)	Si (µg/l)	P (µg/l)	S (µg/l)	Cl (µg/l)	K (µg/l)	Ca (µg/l)	Sc (µg/l)	Ti (µg/l)	V (µg/l)	Cr (µg/l)	Mn (µg/l)	Fe (µg/l)
I1	1.00	<LOD	1.62	3434.31	11052.42	3.61	647.98	1.31	16690.10	5248.35	1365.51	31872.85	0.018	0.065	0.049	0.064	0.09	1.61
I2	1.73	<LOD	2.07	3199.80	10081.91	3.15	935.08	1.06	5925.26	5661.96	1539.97	32348.04	0.023	0.048	0.060	0.086	0.05	0.74
L1	0.78	<LOD	2.48	3358.27	7559.57	3.22	367.08	3.29	4941.12	6027.01	805.29	24946.09	0.016	0.025	0.020	0.075	1.23	8.04
L2	0.77	<LOD	2.50	3211.87	7365.12	1.92	344.18	0.64	4801.47	5857.16	771.56	25096.73	0.014	0.018	0.018	0.038	0.86	3.69
L3	0.81	<LOD	2.72	3268.22	7405.83	1.96	346.19	0.46	4887.95	5926.88	764.08	26236.04	0.014	0.024	0.018	<LOD	0.81	3.84
L4	0.78	<LOD	2.54	3374.02	7581.77	1.50	365.97	0.55	4890.12	5905.39	772.59	25696.37	0.014	0.026	0.014	0.039	0.67	4.42
L5	0.83	<LOD	2.70	3375.49	7633.07	1.28	419.19	0.68	4908.15	6033.02	782.97	26587.88	0.015	0.026	0.017	0.055	10.06	5.39
L6	0.80	<LOD	3.03	3336.25	7538.76	1.10	459.83	0.53	4930.36	6028.38	773.38	26976.02	0.015	0.023	0.015	0.049	9.17	4.86
O1	0.86	<LOD	2.43	3391.76	7621.81	2.28	366.07	0.52	5105.27	6167.06	805.11	26235.97	0.015	0.046	0.024	0.016	0.17	2.75
O2	0.80	<LOD	2.53	3212.42	7284.46	2.25	360.58	0.52	4898.62	5877.30	770.17	24146.11	0.014	0.033	0.031	0.052	0.11	2.70
O3	0.81	<LOD	2.75	3411.70	8053.48	2.62	395.24	0.52	5418.20	6246.74	836.57	25809.15	0.014	0.027	0.035	0.034	0.07	1.77
O4	0.87	<LOD	2.75	3357.45	8093.27	2.62	408.21	0.48	5470.47	6051.19	854.36	25383.07	0.015	0.030	0.033	0.085	0.02	1.18
O5	1.07	<LOD	2.37	3322.13	8418.52	3.15	449.64	0.74	6233.80	5904.05	859.74	28168.94	0.016	0.032	0.033	0.058	0.02	0.72
O6	1.19	<LOD	2.80	3503.45	9044.13	3.38	510.99	0.65	6884.28	6002.94	932.85	28367.94	0.017	0.027	0.060	0.46	0.06	4.26
O7	0.99	<LOD	2.49	3279.59	8481.44	3.19	449.87	0.59	6384.86	5793.44	847.87	27194.21	0.016	0.032	0.037	0.060	<LOD	0.61
O8	1.12	<LOD	2.75	3574.30	9316.80	3.21	496.74	1.05	7101.35	6189.69	965.16	28604.95	0.017	0.037	0.041	0.040	0.01	0.42
N1	2.14	<LOD	3.11	4122.29	11190.13	1.55	1083.47	0.75	10570.62	6141.45	1828.32	43976.59	0.025	0.038	0.063	0.059	0.03	0.84
N2	2.03	<LOD	2.95	4161.30	10744.57	1.48	1089.69	0.97	10903.64	6344.60	1764.48	41063.52	0.024	0.057	0.047	0.073	0.07	1.35
N3	2.17	<LOD	2.89	4147.09	11149.84	1.49	1080.50	1.39	10862.19	6114.49	1788.49	42508.27	0.023	0.041	0.045	0.052	0.03	0.79
N4	2.34	<LOD	3.38	4225.74	11801.56	1.69	1045.65	0.99	11249.79	6270.87	1787.76	41573.18	0.024	0.050	0.055	0.046	0.12	0.57

Sample	Co (µg/l)	Ni (µg/l)	Cu (µg/l)	Zn (µg/l)	Ga (µg/l)	As (µg/l)	Se (µg/l)	Br (µg/l)	Rb (µg/l)	Sr (µg/l)	Y (µg/l)	Zr (µg/l)	Nb (µg/l)	Mo (µg/l)	Cd (µg/l)	In (µg/l)
I1	0.031	0.28	0.85	0.83	0.0033	0.10	<LOD	19.45	0.09	28.63	0.012	0.00054	<LOD	0.18	0.00047	0.00015
I2	0.026	0.23	0.60	0.71	0.0059	0.13	0.14	28.90	0.15	27.04	0.0085	0.0010	0.00022	0.39	0.00073	<LOD
L1	0.024	0.28	17.07	27.17	0.0029	0.15	0.063	26.56	0.50	21.66	0.0049	0.00072	<LOD	0.16	0.010	0.00027
L2	0.014	0.21	6.45	8.78	0.0027	0.15	0.075	26.74	0.47	21.55	0.0033	<LOD	<LOD	0.15	0.0045	<LOD
L3	0.017	0.20	5.03	7.09	0.0031	0.15	0.080	26.80	0.47	22.57	0.0036	<LOD	<LOD	0.15	0.0055	<LOD
L4	0.017	0.20	3.23	5.32	0.0024	0.16	0.075	26.24	0.48	22.52	0.0021	<LOD	<LOD	0.15	0.0046	<LOD
L5	0.018	0.22	6.12	8.21	0.0022	0.18	0.070	27.21	0.49	22.99	0.0024	<LOD	<LOD	0.16	0.0062	<LOD
L6	0.017	0.22	2.06	4.74	<LOD	0.19	0.055	28.84	0.51	23.28	0.0020	<LOD	<LOD	0.14	0.0043	<LOD
O1	0.012	0.17	0.33	0.63	0.0035	0.13	0.079	27.35	0.51	22.85	0.0047	<LOD	<LOD	0.16	0.00072	<LOD
O2	0.014	0.16	0.31	1.59	0.0044	0.12	0.052	26.75	0.47	22.05	0.0054	0.0011	<LOD	0.16	0.00087	<LOD
O3	0.018	0.19	0.31	1.22	0.0045	0.12	0.072	27.45	0.50	23.66	0.0052	<LOD	<LOD	0.15	0.00089	<LOD
O4	0.016	0.17	0.29	0.65	0.0051	0.10	0.073	28.11	0.54	22.93	0.0050	<LOD	<LOD	0.15	0.0024	<LOD
O5	0.014	0.17	0.29	0.72	0.0052	0.10	0.059	27.08	0.55	26.30	0.0050	0.00082	<LOD	0.13	0.00033	<LOD
O6	0.018	0.19	0.47	0.76	0.0047	0.083	0.071	29.41	0.56	27.24	0.0054	<LOD	<LOD	0.14	0.0016	<LOD
O7	0.019	0.17	0.27	0.44	0.0056	0.083	0.063	26.75	0.51	26.25	0.0053	0.00075	<LOD	0.13	0.00088	<LOD
O8	0.019	0.19	0.36	1.08	0.0054	0.080	0.077	29.03	0.58	27.65	0.0059	0.00059	<LOD	0.14	0.0015	<LOD
N1	0.033	0.31	0.68	0.56	0.0036	0.093	0.066	30.57	0.57	49.65	0.013	0.00073	<LOD	0.22	0.0017	<LOD
N2	0.034	0.30	0.64	0.71	0.0028	0.083	0.054	31.12	0.54	45.16	0.010	0.0011	<LOD	0.20	0.00087	<LOD
N3	0.032	0.28	0.59	1.06	0.0028	0.086	0.091	30.14	0.65	46.10	0.010	0.00063	<LOD	0.19	0.00073	<LOD
N4	0.042	0.30	0.64	0.57	0.0034	0.069	0.099	30.11	0.73	46.77	0.011	0.0013	0.00019	0.16	0.0014	<LOD

Sample	Sn (µg/l)	Sb (µg/l)	Cs (µg/l)	Ba (µg/l)	La (µg/l)	Ce (µg/l)	Pr (µg/l)	Nd (µg/l)	Sm (µg/l)	Eu (µg/l)	Gd (µg/l)	Tb (µg/l)	Dy (µg/l)	Ho (µg/l)	Er (µg/l)	Tm (µg/l)	Yb (µg/l)
I1	<LOD	0.011	<LOD	15.54	0.0078	0.0073	0.0022	0.010	0.0031	0.0030	0.0019	0.00035	0.0023	0.00055	0.00097	<LOD	0.0010
I2	<LOD	0.025	<LOD	11.55	0.0047	0.0043	0.0011	0.0049	0.0014	0.0021	0.0012	0.00031	0.00073	0.00037	0.00033	<LOD	0.0010
L1	0.016	0.021	<LOD	7.25	0.0024	0.0032	0.00044	0.0026	<LOD	0.0016	<LOD	0.00010	0.00032	<LOD	<LOD	<LOD	<LOD
L2	<LOD	0.013	<LOD	6.97	0.0014	0.0010	0.00022	0.0013	<LOD	0.0009	<LOD	<LOD	<LOD	<LOD	0.00037	<LOD	<LOD
L3	<LOD	0.020	<LOD	6.96	0.0012	0.00093	0.00025	0.0010	<LOD	0.0014	<LOD	<LOD	0.00058	<LOD	<LOD	<LOD	<LOD
L4	<LOD	0.016	<LOD	6.94	0.00073	0.00041	<LOD	0.0010	<LOD	0.0010	<LOD	<LOD	0.00033	<LOD	<LOD	<LOD	<LOD
L5	<LOD	0.017	<LOD	7.25	0.00075	0.00073	0.00012	0.00093	<LOD	0.0014	<LOD	<LOD	<LOD	<LOD	<LOD	<LOD	<LOD
L6	<LOD	0.020	<LOD	7.69	0.00081	0.0010	0.00015	0.00052	<LOD	0.0010	<LOD	<LOD	<LOD	<LOD	<LOD	<LOD	<LOD
O1	<LOD	0.016	<LOD	7.07	0.0024	0.00053	0.00058	0.0027	<LOD	0.0013	<LOD	0.00015	0.00065	<LOD	0.00073	<LOD	<LOD
O2	<LOD	0.014	<LOD	7.05	0.0028	0.00080	0.00061	0.0035	<LOD	0.0016	0.00054	<LOD	0.00047	<LOD	0.00038	<LOD	<LOD
O3	<LOD	0.023	<LOD	7.90	0.0030	0.0011	0.00078	0.0031	<LOD	0.0018	0.00065	0.00013	<LOD	<LOD	<LOD	<LOD	<LOD
O4	<LOD	0.030	<LOD	8.59	0.0024	0.0014	0.00071	0.0029	<LOD	0.0013	0.00055	0.00010	0.00074	<LOD	0.00028	<LOD	<LOD
O5	<LOD	0.027	<LOD	9.27	0.0028	0.0010	0.00073	0.0029	<LOD	0.0020	0.00085	<LOD	0.00040	<LOD	<LOD	<LOD	<LOD
O6	<LOD	0.023	<LOD	10.30	0.0029	0.0019	0.00078	0.0020	<LOD	0.0019	0.0010	0.00013	0.0012	<LOD	<LOD	<LOD	<LOD
O7	<LOD	0.023	<LOD	9.65	0.0026	0.0010	0.00039	0.0025	<LOD	0.0015	<LOD	<LOD	<LOD	<LOD	0.00027	<LOD	<LOD
O8	<LOD	0.029	<LOD	10.57	0.0030	0.0011	0.00061	0.0024	0.0018	0.0013	0.00077	0.00017	0.00055	<LOD	0.00028	<LOD	<LOD
N1	0.0045	0.019	<LOD	18.88	0.0065	0.0032	0.0019	0.0056	0.0014	0.0029	0.00087	0.00030	0.0013	0.00024	0.00092	0.00021	0.0012
N2	<LOD	0.024	<LOD	16.52	0.0050	0.0028	0.0012	0.0070	0.0011	0.0025	0.0025	0.00026	0.0011	0.00028	0.00069	<LOD	<LOD
N3	<LOD	0.024	<LOD	16.83	0.0053	0.0026	0.00098	0.0054	0.0014	0.0037	0.0011	0.00029	0.0010	0.00018	0.00053	<LOD	0.0011
N4	<LOD	0.029	0.0066	16.44	0.0052	0.0028	0.0018	0.0079	0.0015	0.0031	0.00073	0.00054	0.0015	0.00043	0.0012	0.00047	<LOD

Sample	Lu (µg/l)	Hf (µg/l)	Ta (µg/l)	W (µg/l)	Pt (µg/l)	Hg (µg/l)	Tl (µg/l)	Pb (µg/l)	Bi (µg/l)	Th (µg/l)	U (µg/l)
I1	<LOD	<LOD	<LOD	<LOD	<LOD	0.015	<LOD	<LOD	<LOD	<LOD	0.039
I2	<LOD	<LOD	<LOD	<LOD	<LOD	0.017	<LOD	<LOD	<LOD	<LOD	0.25
L1	<LOD	0.00067	<LOD	0.0017	<LOD	0.019	<LOD	0.55	<LOD	<LOD	0.21
L2	<LOD	<LOD	<LOD	0.0012	<LOD	<LOD	<LOD	0.17	<LOD	<LOD	0.20
L3	<LOD	<LOD	<LOD	0.0017	<LOD	<LOD	<LOD	0.15	<LOD	<LOD	0.21
L4	<LOD	0.00081	<LOD	<LOD	<LOD	<LOD	<LOD	0.056	<LOD	<LOD	0.20
L5	<LOD	0.00068	<LOD	<LOD	<LOD	<LOD	<LOD	0.043	<LOD	<LOD	0.20
L6	<LOD	<LOD	<LOD	<LOD	<LOD	<LOD	<LOD	0.019	<LOD	<LOD	0.20
O1	<LOD	<LOD	<LOD	<LOD	<LOD	<LOD	<LOD	<LOD	0.019	<LOD	0.22
O2	<LOD	0.00082	<LOD	0.0020	<LOD	0.016	<LOD	<LOD	<LOD	<LOD	0.19
O3	<LOD	<LOD	<LOD	0.0014	<LOD	<LOD	<LOD	<LOD	<LOD	<LOD	0.22
O4	<LOD	<LOD	<LOD	<LOD	<LOD	<LOD	<LOD	<LOD	<LOD	<LOD	0.21
O5	<LOD	<LOD	<LOD	<LOD	<LOD	<LOD	<LOD	<LOD	<LOD	<LOD	0.22
O6	<LOD	<LOD	<LOD	<LOD	<LOD	<LOD	<LOD	<LOD	<LOD	<LOD	0.27
O7	<LOD	<LOD	<LOD	0.0023	<LOD	<LOD	<LOD	<LOD	<LOD	<LOD	0.24
O8	<LOD	<LOD	<LOD	<LOD	<LOD	<LOD	<LOD	<LOD	<LOD	<LOD	0.26
N1	<LOD	0.00070	<LOD	0.0015	<LOD	<LOD	<LOD	<LOD	<LOD	<LOD	0.48
N2	<LOD	<LOD	<LOD	<LOD	<LOD	<LOD	<LOD	<LOD	<LOD	<LOD	0.48
N3	<LOD	<LOD	<LOD	0.0019	<LOD	<LOD	<LOD	<LOD	<LOD	<LOD	0.48
N4	0.00037	<LOD	<LOD	0.0022	<LOD	<LOD	<LOD	<LOD	<LOD	0.0011	0.49

F.2 Unfiltered water samples

Raw data from laboratory analyses on unfiltered water samples collected at Ossian Sars on August 18th (I1, I2, L1-L6 and O1-O6) and August 19th, 2021 (O7, O8 and N1-N4).

Sample	Li (µg/l)	Be (µg/l)	B (µg/l)	Na (µg/l)	Mg (µg/l)	Al (µg/l)	Si (µg/l)	P (µg/l)	S (µg/l)	Cl (µg/l)	K (µg/l)	Ca (µg/l)	Sc (µg/l)	Ti (µg/l)	V (µg/l)	Cr (µg/l)	Mn (µg/l)
I1	0.92	0.0017	1.16	3282.13	10238.63	22.31	687.11	2.51	15982.83	4132.24	1398.49	31774.07	0.025	1.82	0.084	0.067	0.49
I2	1.62	<LOD	1.39	3153.89	9709.92	6.82	983.48	1.22	5773.44	4464.83	1582.32	34935.69	0.024	0.30	0.060	<LOD	0.12
L1	0.69	<LOD	1.69	3076.30	6814.24	8.33	354.07	2.95	4566.32	4602.95	775.22	26200.83	0.017	0.30	0.033	0.15	13.42
L2	0.67	<LOD	2.03	3137.18	6939.68	5.27	335.75	1.22	4674.73	4592.26	788.76	24934.62	0.018	0.23	0.023	<LOD	12.89
L3	0.68	<LOD	1.79	3152.49	6979.54	5.81	357.82	1.21	4667.86	4661.67	806.32	24929.00	0.019	0.28	0.024	0.053	13.46
L4	0.70	<LOD	1.91	3201.71	7080.96	5.74	382.59	1.72	4750.82	4912.93	804.84	26394.47	0.019	0.36	0.027	0.065	30.84
L5	0.71	0.0024	1.99	3255.33	7204.56	5.63	474.70	1.46	4806.01	4855.11	813.72	26411.77	0.017	0.33	0.026	<LOD	62.77
L6	0.86	0.011	2.35	3276.48	7305.53	150.19	696.53	4.41	4915.86	4731.36	881.44	27035.01	0.035	15.55	0.35	0.24	85.83
O1	0.76	<LOD	2.06	3238.65	7111.40	2.07	364.40	0.62	4897.67	4832.98	824.84	25703.30	0.018	0.026	0.020	<LOD	0.19
O2	0.73	<LOD	1.71	3192.68	7142.57	4.91	357.48	0.82	4799.70	4815.96	803.48	25864.99	0.016	0.22	0.033	<LOD	0.71
O3	0.80	<LOD	2.17	3202.60	7390.29	5.92	1082.87	0.96	5102.59	4722.96	824.35	26606.85	0.018	0.25	0.036	<LOD	0.35
O4	0.86	<LOD	1.88	3260.81	7645.29	5.39	418.58	0.72	5359.22	4957.83	859.28	26562.09	0.018	0.20	0.035	0.033	0.10
O5	0.94	<LOD	2.03	3381.60	8338.96	4.36	486.49	0.66	6289.22	4911.17	904.36	28633.73	0.020	0.12	0.033	<LOD	<LOD
O6	1.09	0.0018	2.17	3385.85	8504.93	35.39	555.45	1.55	6665.10	4913.20	968.05	29370.57	0.023	3.02	0.11	0.13	0.76
O7	1.02	<LOD	1.61	3297.93	8238.51	5.14	535.59	1.64	6380.35	4807.64	908.78	30104.97	0.018	0.13	0.035	<LOD	<LOD
O8	1.01	<LOD	2.12	3332.87	8584.87	4.49	539.44	0.72	6643.63	4870.34	915.51	27310.52	0.021	0.13	0.037	<LOD	0.042
N1	2.02	<LOD	2.05	4020.39	10706.82	2.71	1130.09	0.92	10212.26	4876.99	1856.56	44580.68	0.030	0.091	0.056	<LOD	0.029
N2	1.83	<LOD	2.30	4113.75	10307.98	3.61	1153.42	1.22	10435.76	4911.35	1771.56	41628.74	0.030	0.19	0.051	<LOD	0.092
N3	2.00	<LOD	2.40	4130.72	10858.01	3.90	1177.82	2.26	10700.43	5151.21	1853.68	42262.21	0.027	0.19	0.049	0.087	0.068
N4	1.98	<LOD	2.90	4169.03	11505.58	2.64	1136.63	1.19	11120.57	5115.67	1859.96	42803.97	0.028	0.095	0.044	<LOD	0.010

Sample	Fe (μg/l)	Co (μg/l)	Ni (μg/l)	Cu (μg/l)	Zn (μg/l)	Ga (μg/l)	As (μg/l)	Se (μg/l)	Br (μg/l)	Rb (μg/l)	Sr (μg/l)	Y (μg/l)	Zr (μg/l)	Nb (μg/l)	Mo (μg/l)	Cd (μg/l)	In (μg/l)
I1	27.61	0.042	0.32	0.90	1.09	0.0069	0.10	<LOD	17.32	0.16	27.58	0.017	<LOD	0.00083	0.17	0.0028	<LOD
I2	4.70	0.026	0.23	0.55	0.63	0.0052	0.12	<LOD	26.79	0.16	27.59	0.0095	0.00056	<LOD	0.41	0.0016	<LOD
L1	51.72	0.037	0.31	60.74	43.08	<LOD	0.17	<LOD	23.48	0.50	22.15	0.010	0.0033	0.00040	0.16	0.046	0.0023
L2	31.88	0.018	0.24	19.60	14.85	0.0029	0.17	<LOD	24.73	0.49	21.50	0.0071	0.0024	<LOD	0.14	0.014	0.00063
L3	33.51	0.024	0.22	16.52	11.16	0.0025	0.16	<LOD	24.81	0.49	21.06	0.0068	0.00090	<LOD	0.15	0.015	<LOD
L4	50.61	0.031	0.24	9.08	7.73	0.0018	0.18	<LOD	24.07	0.51	21.74	0.0070	0.00074	<LOD	0.16	0.011	<LOD
L5	74.16	0.041	0.25	17.20	11.82	<LOD	0.20	<LOD	28.07	0.53	22.24	0.0064	<LOD	0.00046	0.15	0.0087	<LOD
L6	313.93	0.16	0.40	7.67	7.37	0.055	0.22	<LOD	26.85	1.00	22.37	0.040	0.0039	0.031	0.13	0.021	0.00052
O1	2.98	0.011	0.17	0.30	0.52	<LOD	0.13	<LOD	26.09	0.53	22.10	0.0054	<LOD	<LOD	0.15	0.0012	<LOD
O2	8.51	0.013	0.16	0.29	1.28	0.0017	0.12	<LOD	26.36	0.50	21.52	0.0063	<LOD	<LOD	0.16	0.0028	<LOD
O3	8.64	0.014	0.17	0.32	0.81	<LOD	0.11	<LOD	26.46	0.50	22.76	0.0062	<LOD	<LOD	0.14	0.0028	<LOD
O4	4.60	0.013	0.19	0.27	0.42	0.0018	0.10	<LOD	26.34	0.56	23.20	0.0052	<LOD	<LOD	0.14	0.0018	<LOD
O5	1.76	0.014	0.18	0.25	0.35	0.0033	0.084	<LOD	26.26	0.57	26.02	0.0057	<LOD	<LOD	0.14	0.00087	<LOD
O6	47.68	0.032	0.24	0.42	1.00	0.015	0.071	<LOD	26.05	0.68	27.10	0.015	<LOD	0.0014	0.14	0.0016	<LOD
O7	2.02	0.015	0.19	0.27	1.47	0.0048	0.070	<LOD	28.52	0.56	27.16	0.0050	<LOD	<LOD	0.11	0.0010	<LOD
O8	2.36	0.015	0.18	2.59	1.18	0.0029	0.069	<LOD	27.05	0.55	25.21	0.0057	<LOD	<LOD	0.14	<LOD	<LOD
N1	1.98	0.028	0.31	0.66	0.45	0.0051	0.066	<LOD	30.09	0.58	47.75	0.012	<LOD	<LOD	0.22	0.0010	<LOD
N2	3.71	0.031	0.30	0.63	1.18	0.0019	0.054	<LOD	32.63	0.55	44.50	0.012	<LOD	<LOD	0.19	0.00070	<LOD
N3	4.15	0.031	0.32	0.65	2.10	0.0029	0.073	<LOD	30.09	0.70	46.08	0.011	<LOD	<LOD	0.18	0.0014	<LOD
N4	1.43	0.032	0.31	0.63	0.44	<LOD	0.075	<LOD	29.62	0.75	45.83	0.010	<LOD	<LOD	0.18	0.0012	<LOD

Sample	Sn (µg/l)	Sb (µg/l)	Cs (µg/l)	Ba (µg/l)	La (µg/l)	Ce (µg/l)	Pr (µg/l)	Nd (µg/l)	Sm (µg/l)	Eu (µg/l)	Gd (µg/l)	Tb (µg/l)	Dy (µg/l)	Ho (µg/l)	Er (µg/l)	Tm (µg/l)	Yb (µg/l)
I1	<LOD	<LOD	0.0034	14.85	0.012	0.015	0.0036	0.015	0.0027	0.0043	0.0024	0.00066	0.0021	0.00023	0.0013	<LOD	<LOD
I2	<LOD	0.017	<LOD	11.22	0.0059	0.0067	0.0012	0.0071	0.0011	0.0023	0.0018	<LOD	0.0011	<LOD	0.00078	<LOD	<LOD
L1	0.12	0.026	<LOD	8.15	0.0090	0.012	0.0019	0.0077	0.0015	0.0020	0.0017	<LOD	<LOD	<LOD	0.00065	<LOD	<LOD
L2	0.042	0.016	<LOD	7.31	0.0060	0.0071	0.0013	0.0067	0.0010	0.0015	0.0013	<LOD	0.00061	<LOD	0.00060	<LOD	<LOD
L3	0.032	0.014	<LOD	7.52	0.0061	0.0074	0.0014	0.0080	0.0015	0.0016	0.00036	<LOD	0.00084	<LOD	0.00060	<LOD	<LOD
L4	0.016	0.016	<LOD	7.13	0.0058	0.0074	0.0010	0.0045	0.0014	0.0014	0.0012	<LOD	0.00031	<LOD	0.00030	<LOD	<LOD
L5	0.021	0.025	<LOD	7.37	0.0041	0.0062	0.0010	0.0049	0.00060	0.0010	0.0012	<LOD	0.0012	<LOD	0.00085	<LOD	<LOD
L6	0.023	0.026	0.040	9.09	0.057	0.11	0.014	0.0544	0.013	0.0037	0.012	0.0012	0.0093	0.0016	0.0037	0.00036	0.0044
O1	<LOD	0.013	<LOD	7.05	0.0021	0.00068	0.00048	0.0022	0.00048	0.00089	0.00072	<LOD	0.00061	<LOD	0.00018	<LOD	<LOD
O2	<LOD	0.015	<LOD	6.84	0.0045	0.0028	0.00083	0.0034	0.00058	0.0012	0.0011	<LOD	0.000073	<LOD	0.00012	<LOD	<LOD
O3	0.030	0.025	<LOD	7.49	0.0045	0.0033	0.00082	0.0045	0.0012	0.0010	0.00084	<LOD	0.00031	<LOD	0.00042	<LOD	<LOD
O4	<LOD	0.024	<LOD	8.39	0.0038	0.0026	0.00074	0.0034	0.00084	0.0019	0.00072	<LOD	0.000075	<LOD	0.00036	<LOD	<LOD
O5	<LOD	0.024	0.0024	9.26	0.0037	0.0018	0.00089	0.0026	0.00059	0.0015	0.00083	<LOD	0.000076	<LOD	0.00041	<LOD	<LOD
O6	<LOD	0.021	0.0094	9.99	0.015	0.024	0.0041	0.018	0.0026	0.0031	0.0045	0.00028	0.0026	0.00059	0.0014	<LOD	<LOD
O7	<LOD	0.023	<LOD	10.52	0.0031	0.0025	0.00065	0.0039	0.0013	0.0013	0.00024	<LOD	0.00053	<LOD	0.00047	<LOD	<LOD
O8	<LOD	0.020	<LOD	9.83	0.0040	0.0022	0.00047	0.0036	0.00071	0.0020	0.00059	<LOD	0.00046	<LOD	0.00047	<LOD	<LOD
N1	<LOD	0.015	<LOD	17.30	0.0058	0.0039	0.0016	0.0074	0.0027	0.0029	0.0019	<LOD	0.0018	0.00031	0.00059	<LOD	0.0012
N2	<LOD	0.025	<LOD	16.44	0.0060	0.0048	0.0017	0.0066	0.0025	0.0026	0.0011	<LOD	0.0013	<LOD	0.0011	<LOD	<LOD
N3	<LOD	0.027	0.0037	18.10	0.0057	0.0038	0.0014	0.0059	0.0011	0.0032	0.0011	<LOD	0.0018	0.00022	0.00090	<LOD	<LOD
N4	<LOD	0.030	0.0068	16.54	0.0055	0.0033	0.0011	0.0059	0.0019	0.0032	0.0018	<LOD	0.00046	<LOD	0.00066	<LOD	0.0012

Sample	Lu (µg/l)	Hf (µg/l)	Ta (µg/l)	W (µg/l)	Pt (µg/l)	Hg (µg/l)	Tl (µg/l)	Pb (µg/l)	Bi (µg/l)	Th (µg/l)	U (µg/l)
I1	0.00019	<LOD	<LOD	<LOD	<LOD	<LOD	<LOD	<LOD	0.00081	<LOD	0.039
I2	<LOD	<LOD	<LOD	<LOD	<LOD	<LOD	<LOD	<LOD	<LOD	<LOD	0.29
L1	0.00015	<LOD	<LOD	0.0063	<LOD	<LOD	0.0017	2.70	0.0048	0.0022	0.20
L2	0.00017	<LOD	<LOD	<LOD	<LOD	<LOD	0.0013	1.03	0.0018	0.00063	0.20
L3	0.000087	<LOD	<LOD	<LOD	<LOD	<LOD	<LOD	0.90	0.0014	<LOD	0.21
L4	0.000044	<LOD	0.00014	<LOD	<LOD	<LOD	<LOD	0.57	<LOD	0.00064	0.23
L5	0.000087	<LOD	0.00014	<LOD	<LOD	<LOD	0.0020	0.61	0.0031	0.00064	0.20
L6	0.00021	<LOD	0.00028	<LOD	<LOD	<LOD	0.0051	0.94	0.0035	0.0019	0.23
O1	<LOD	<LOD	<LOD	<LOD	<LOD	<LOD	0.0013	<LOD	<LOD	<LOD	0.25
O2	<LOD	<LOD	<LOD	<LOD	<LOD	<LOD	0.0015	<LOD	<LOD	<LOD	0.23
O3	<LOD	<LOD	<LOD	<LOD	<LOD	<LOD	0.0015	<LOD	<LOD	<LOD	0.23
O4	<LOD	<LOD	<LOD	<LOD	<LOD	<LOD	<LOD	<LOD	<LOD	<LOD	0.26
O5	<LOD	<LOD	<LOD	<LOD	<LOD	<LOD	<LOD	<LOD	<LOD	<LOD	0.27
O6	0.00017	<LOD	<LOD	<LOD	<LOD	<LOD	<LOD	<LOD	<LOD	0.0013	0.33
O7	<LOD	<LOD	<LOD	<LOD	<LOD	<LOD	<LOD	<LOD	<LOD	<LOD	0.33
O8	<LOD	<LOD	<LOD	<LOD	<LOD	<LOD	<LOD	<LOD	<LOD	<LOD	0.30
N1	0.00015	<LOD	<LOD	<LOD	<LOD	<LOD	<LOD	<LOD	<LOD	<LOD	0.63
N2	<LOD	<LOD	<LOD	<LOD	<LOD	<LOD	<LOD	<LOD	<LOD	0.00065	0.52
N3	<LOD	<LOD	<LOD	<LOD	<LOD	<LOD	<LOD	<LOD	<LOD	<LOD	0.53
N4	0.00015	<LOD	<LOD	<LOD	<LOD	<LOD	0.0021	<LOD	<LOD	<LOD	0.56

F.3 Detection limits ICP-MS

Detection limits (LOD for elements in water samples analyzed by ICP-MS.

Name	LOD (µg/l)	Name	LOD (µg/l)	Name	LOD (µg/l)
Li	0.0071	**Zn**	0.0040	**Sm**	0.0003
Be	0.0008	**Ga**	0.0007	**Eu**	0.0001
B	0.1395	**As**	0.0021	**Gd**	0.0002
Na	0.3084	**Se**	0.0178	**Tb**	0.0000
Mg	0.0027	**Br**	0.0367	**Dy**	0.0001
Al	0.0013	**Rb**	0.0034	**Ho**	0.0001
Si	0.0553	**Sr**	0.0006	**Er**	0.0001
P	0.0243	**Y**	0.0000	**Tm**	0.0001
S	0.0934	**Zr**	0.0002	**Yb**	0.0003
Cl	51.1845	**Nb**	0.0001	**Lu**	0.0001
K	0.0691	**Mo**	0.0010	**Hf**	0.0002
Ca	0.1298	**Cd**	0.0000	**Ta**	0.0001
Sc	0.0004	**In**	0.0000	**W**	0.0004
Ti	0.0006	**Sn**	0.0012	**Pt**	0.0011
V	0.0012	**Sb**	0.0004	**Hg**	0.0043
Cr	0.0041	**Cs**	0.0011	**Tl**	0.0008
Mn	0.0022	**Ba**	0.0006	**Pb**	0.0036
Fe	0.0059	**La**	0.0001	**Bi**	0.0001
Co	0.0006	**Ce**	0.0001	**Th**	0.0003
Ni	0.0103	**Pr**	0.0000	**U**	0.0001
Cu	0.0063	**Nd**	0.0001		

Appendix G. – Ion and nutrient data

G.1 Ions and nutrients raw data

Ion and nutrient primary data from laboratory analyses on water samples collected from Ossian Sars on August 18th and 19th 2021.

Sample	**TP [µg/l]**	**TN [mg/l]**	**NH_4-N [µg/l]**	**NO_3^- [mg/l]**	**F^- [mg/l]**	**NO_2^- [mg/l]**	**SO_4^{2-} [mg/l]**	**Cl^- [mg/l]**	**PO_4^{3-} [mg/l]**	**Br^- [mg/l]**
I1	7	0.54	52	1.06	<LOD	<LOD	33.6	4.8	<LOD	<LOD
I2	8	0.67	<LOD	2.35	<LOD	<LOD	15.9	5.2	<LOD	<LOD
L1	7	0.25	<LOD	0.21	<LOD	<LOD	12.6	5.4	<LOD	<LOD
L2	6	0.20	24	0.21	<LOD	<LOD	13.3	5.6	<LOD	<LOD
L3	6	<LOD	<LOD	0.26	0.20	<LOD	12.5	5.6	<LOD	<LOD
L4	6	<LOD	<LOD	0.23	0.19	<LOD	12.6	5.7	<LOD	<LOD
L5	6	<LOD	<LOD	0.19	<LOD	<LOD	13.1	5.7	<LOD	<LOD
L6	8	0.27	<LOD	0.18	<LOD	<LOD	13.1	5.6	<LOD	<LOD
O1	N/A	N/A	N/A	N/A	N/A	N/A	N/A	N/A	N/A	N/A
O2	6	<LOD	<LOD	0.23	<LOD	<LOD	12.8	5.5	<LOD	<LOD
O3	5	<LOD	<LOD	0.30	<LOD	0.172	13.4	5.4	<LOD	<LOD
O4	5	<LOD	<LOD	0.51	<LOD	<LOD	15.2	5.4	<LOD	<LOD
O5	N/A	0.25	<LOD	0.55	<LOD	<LOD	16.3	5.5	<LOD	<LOD
O6	N/A	N/A	N/A	0.59	<LOD	<LOD	16.4	5.3	<LOD	<LOD
O7	8	0.37	25	0.56	<LOD	<LOD	16.5	5.5	<LOD	<LOD
O8	7	0.40	<LOD	0.58	<LOD	<LOD	16.5	5.4	<LOD	<LOD
N1	5	0.41	<LOD	1.06	<LOD	<LOD	24.1	5.5	<LOD	<LOD
N2	5	0.48	<LOD	1.08	<LOD	<LOD	23.9	5.8	<LOD	<LOD
N3	6	0.47	<LOD	1.51	<LOD	<LOD	24.4	5.9	<LOD	<LOD
N4	5	0.45	22	1.21	<LOD	<LOD	25.0	5.7	<LOD	<LOD

G.2 Non-sea-salt ion concentrations

Non-sea-salt (nss) ion concentrations (mg/l) in filtered water samples at Ossian Sars.

Sample	$nssSO_4^{2-}$		$nssCa^{2+}$		$nssMg^{2+}$		$nssK^{+}$		$nssNa^{+}$	
	mg/l	% of total	mg/l	% of total	mg/l	% of total	mg/l	% of total	mg/l	% of total
I1	33.1	98.5	31.7	99.4	10.1	91.5	1.3	93.3	-0.7	-20.2
I2	15.4	96.6	32.2	99.4	9.1	89.9	1.4	93.6	-1.3	-39.8
L1	12.0	95.6	24.7	99.2	6.5	86.2	0.7	87.4	-1.3	-37.2
L2	12.7	95.6	24.9	99.1	6.3	85.1	0.7	86.2	-1.6	-50.4
L3	12.0	95.4	26.0	99.2	6.3	85.3	0.7	86.2	-1.5	-46.4
L4	12.0	95.3	25.5	99.2	6.5	85.4	0.7	86.0	-1.5	-45.0
L5	12.5	95.5	26.4	99.2	6.5	85.5	0.7	86.2	-1.5	-44.9
L6	12.5	95.6	26.8	99.2	6.4	85.5	0.7	86.3	-1.5	-44.2
O1	N/A	N/A	N/A	N/A	N/A	N/A	N/A	N/A	N/A	N/A
O2	12.3	95.6	23.9	99.1	6.2	85.4	0.7	86.5	-1.5	-46.5
O3	12.8	95.8	25.6	99.2	7.0	86.9	0.7	87.7	-1.2	-36.4
O4	14.6	96.4	25.2	99.2	7.0	87.1	0.8	88.1	-1.3	-37.5
O5	15.8	96.5	28.0	99.3	7.3	87.3	0.8	87.9	-1.4	-42.3
O6	15.8	96.7	28.2	99.3	8.0	88.6	0.8	89.2	-1.1	-30.3
O7	16.0	96.6	27.0	99.2	7.4	87.4	0.7	87.7	-1.4	-44.0
O8	16.0	96.6	28.4	99.3	8.3	88.7	0.9	89.4	-1.1	-29.9
N1	23.5	97.6	43.8	99.5	10.1	90.4	1.7	94.2	-0.6	-15.5
N2	23.3	97.5	40.8	99.5	9.6	89.5	1.7	93.8	-0.8	-19.7
N3	23.8	97.5	42.3	99.5	10.0	89.7	1.7	93.7	-0.9	-22.5
N4	24.4	97.7	41.4	99.5	10.7	90.7	1.7	94.0	-0.6	-15.1

Appendix H. – PCA

H.1 Eigenvalues

Eigenvalues for the variables included in the PCA on filtered water samples.

	PC1	PC2	PC3	PC4	PC5	PC6	PC7
Cd	0,02	0,21	-0,17	0,68	0,10	-0,44	-0,40
Zn	-0,11	-0,03	0,39	-0,25	0,63	-0,47	0,07
Ni	0,31	-0,11	0,04	0,00	0,00	-0,11	0,00
As	-0,18	-0,14	0,28	-0,31	-0,44	-0,43	-0,15
Cu	0,26	-0,28	0,00	0,03	-0,05	-0,26	0,22
Co	0,31	-0,08	0,00	-0,01	0,05	-0,06	-0,03
Fe	-0,14	-0,11	0,37	0,49	-0,01	0,03	0,65
Mn	-0,01	-0,23	0,54	0,21	-0,32	0,24	-0,23
Al	-0,20	-0,21	-0,43	0,01	0,02	-0,05	0,39
Cl^-	0,15	0,38	0,21	-0,16	0,21	0,31	0,02
Br	0,12	0,44	0,15	0,12	-0,15	-0,14	0,20
Na	0,29	0,11	0,15	0,12	0,17	0,17	-0,06
pH	0,20	0,30	-0,11	-0,09	-0,41	-0,15	0,18
Cond	0,32	0,01	0,01	-0,05	-0,04	-0,01	0,08
TOC	0,15	-0,44	0,01	0,13	0,05	0,02	-0,15
Ca	0,32	0,05	0,06	-0,06	-0,04	-0,03	0,08
Mg	0,31	-0,11	-0,11	-0,02	0,03	-0,10	0,13
SO_4^{2-}	0,25	-0,30	-0,08	0,02	0,13	0,19	-0,07
K	0,31	-0,03	0,05	-0,10	-0,08	-0,20	0,04

	PC8	PC9	PC10	PC11	PC12	PC13	PC14
Cd	-0,06	-0,08	0,03	-0,10	0,17	0,03	0,15
Zn	0,21	-0,17	-0,23	0,07	0,03	-0,03	0,04
Ni	-0,12	0,20	0,09	0,44	-0,34	-0,18	0,07
As	-0,33	0,21	0,17	-0,16	0,26	-0,20	0,14
Cu	-0,04	-0,02	0,01	-0,02	-0,28	0,27	0,46
Co	0,35	-0,07	0,69	0,22	0,07	0,02	-0,02
Fe	-0,28	-0,10	0,15	0,03	0,11	0,00	-0,17
Mn	0,53	-0,06	-0,18	-0,02	0,07	0,09	0,16
Al	0,35	0,15	-0,03	-0,19	0,15	-0,33	0,32
Cl^-	-0,14	-0,23	0,33	-0,36	0,12	-0,16	0,37
Br	0,23	0,37	-0,10	-0,26	-0,36	-0,09	0,10
Na	-0,06	0,37	-0,24	0,10	0,12	-0,45	-0,04
pH	0,07	-0,62	-0,29	0,21	0,06	-0,21	0,03
Cond	-0,04	0,02	-0,01	-0,13	0,18	0,20	0,20
TOC	-0,06	-0,29	0,02	-0,20	-0,16	-0,59	-0,07
Ca	-0,14	0,11	-0,17	0,27	0,35	0,02	0,04
Mg	0,22	0,14	-0,03	-0,16	0,51	0,07	-0,28
SO_4^{2-}	-0,27	-0,05	-0,31	-0,21	0,01	0,22	0,21
K	0,02	-0,06	0,00	-0,48	-0,25	0,08	-0,51

H.2 Importance of components

Table listing the importance of the principal components in the PCA.

	PC1	PC2	PC3	PC4	PC5	PC6	PC7
Standard deviation	3.1066	1.9478	1.3386	1.1018	0.97013	0.78351	0.70655
Proportion of Variance	0.5079	0.1997	0.09431	0.0639	0.04953	0.03231	0.02627
Cumulative Proportion	0.5079	0.7076	0.80192	0.8658	0.91535	0.94766	0.97393

	PC8	PC9	PC10	PC11	PC12	PC13	PC14
Standard deviation	0.49598	0.37644	0.25502	0.14142	0.12612	0.0814	0.0000
Proportion of Variance	0.01295	0.00746	0.00342	0.00105	0.00084	0.00035	0.0000
Cumulative Proportion	0.98688	0.99434	0.99776	0.99881	0.99965	1.0000	1.0000

Appendix I. – Spearman correlation matrix

Spearman correlation matrix showing the strength of the variables' relationship through the correlation coefficients (ρ). The value 1 represents a strong positive correlation and -1 a strong negative correlation. The positive correlations are colored a blue gradient and the negative correlations are colored a red gradient.

	Cd	**Zn**	**Ni**	**As**	**Cu**	**Co**	**Fe**	**Mn**	**Al**	**Cl^-**	**Br**	**Na**	**pH**	**Cond**	**TOC**	**Ca**	**Mg**	**SO_4^{2-}**	**K**
Cd	1.00																		
Zn	-0.19	1.00																	
Ni	0.02	-0.20	1.00																
As	-0.45	0.20	-0.42	1.00															
Cu	-0.02	-0.07	0.89	-0.26	1.00														
Co	0.17	-0.24	0.88	-0.63	0.78	1.00													
Fe	-0.05	0.28	-0.19	0.46	0.03	-0.40	1.00												
Mn	-0.25	0.16	0.16	0.28	0.40	0.02	0.58	1.00											
Al	-0.03	0.17	-0.34	0.06	-0.24	-0.35	-0.03	-0.30	1.00										
Cl^-	0.08	-0.19	0.27	-0.47	0.01	0.42	-0.34	-0.16	-0.74	1.00									
Br	0.41	-0.17	0.67	-0.53	0.49	0.64	-0.14	-0.04	-0.60	0.53	1.00								
Na	0.24	-0.10	0.76	-0.70	0.61	0.71	-0.13	0.17	-0.42	0.50	0.73	1.00							
pH	0.17	-0.53	0.48	-0.33	0.30	0.57	-0.52	-0.31	-0.49	0.57	0.66	0.25	1.00						
Cond	0.03	-0.33	0.87	-0.60	0.78	0.91	-0.40	-0.03	-0.28	0.40	0.65	0.71	0.65	1.00					
TOC	-0.16	-0.20	0.75	-0.11	0.89	0.63	0.21	0.60	-0.41	0.10	0.40	0.57	0.25	0.68	1.00				
Ca	-0.03	-0.28	0.92	-0.47	0.78	0.87	-0.40	-0.06	-0.34	0.40	0.69	0.68	0.68	0.96	0.64	1.00			
Mg	0.08	-0.30	0.89	-0.59	0.79	0.93	-0.46	-0.07	-0.22	0.36	0.60	0.70	0.62	0.98	0.65	0.95	1.00		
SO_4^{2-}	-0.20	-0.39	0.74	-0.46	0.69	0.69	-0.23	0.16	-0.17	0.25	0.30	0.70	0.24	0.80	0.71	0.75	0.79	1.00	
K	0.05	-0.20	0.87	-0.50	0.79	0.87	-0.39	-0.03	-0.42	0.42	0.74	0.69	0.69	0.93	0.68	0.93	0.92	0.65	1.00

Norges miljø- og biovitenskapelige universitet
Noregs miljø- og biovitskapelege universitet
Norwegian University of Life Sciences

Postboks 5003
NO-1432 Ås
Norway